Classification of continuous phase transitions and stable phases. II. Four-dimensional order parameters

Jai Sam Kim, Harold T. Stokes, and Dorian M. Hatch
Department of Physics and Astronomy, Brigham Young University, Provo, Utah 84602
(Received 2 December 1985)

We have classified continuous phase transitions in physical systems where the order parameter transforms as a four-dimensional representation of a three-dimensional space group. For most active four-dimensional space-group representations the "phase diagrams" are obtained. We also give prescriptions to lift the degeneracy, occurring at the fourth-degree polynomical expansion of the free energy, between phases preserving maximal isotropy subgroups and to distinguish images yielding the same quartic potential. In two cases we have found that the symmetry is reduced to the *minimal* one after the phase transition.

I. INTRODUCTION

Recently we classified[1] all possible second-order phase transitions allowed by the Landau theory for physical systems whose order parameter transforms as a six-dimensional representation of a space group. A complete "phase diagram"—a list of stable phases versus regions in the coupling constant space—was obtained for most of the active six-dimensional space-group representations. Out of 43 six-dimensional active representations corresponding to points of symmetry in the Brillouin zone, 32 representations were treated.

The procedure to carry out such a project was detailed in previous works.[2–7] We outline it briefly in the following.

(1) Space-group representations with equivalent images are grouped together (the image of an irreducible representation, irrep, is the set of distinct matrices of the irrep and it forms a finite group).

(2) Landau and Lifshitz conditions (necessary conditions for continuous phase transitions) are imposed to sort out active images.

(3) These active images are further classified according to distinct types of the fourth-degree expansion of the free energy (different images can give rise to the same fourth-degree potential and the largest group that leaves the quartic potential invariant is called the centralizer of the potential).

(4) A complete list of isotropy subgroups and their invariant vectors for each active image is computed.

(5) Each type of fourth-degree potential is minimized in every region of the coupling constant space.

In the last two steps we have been using Kim's minimization technique[8] with the complete table of isotropy subgroups computed by Stokes and Hatch.[9] For further details we refer the reader to Ref. 1 which also contains extensive references. In this way the phase diagrams are readily obtained for potentials consisting of less than five linearly independent fourth-degree invariant polynomials. The minimization becomes quite tedious if there are more than four linearly independent fourth-degree invariant polynomials, though the same procedure[10] is used.

In this paper we carry out the above project for four-dimensional active space-group representations corresponding to points of symmetry in the Brillouin zone. A similar project was carried out by Tolédano and Tolédano,[4] who listed 13 different types of quartic potential complying with both the Landau and Lifshitz conditions. Michel, Tolédano, and Tolédano[11] enumerated all irreducible subgroups of O(4) and found 27 centralizers, 22 of which comply with the Landau condition but not necessarily with the Lifshitz condition. Part of the 27 centralizers are not related to images of space-group representations due to the requirement that the group must comply with the periodicity of a crystal lattice in three dimensions. Recently the effective Hamiltonians with these quartic potentials were further analyzed[12] by renormalization-group methods. It was found that only five Hamiltonians have stable fixed points.

We have found 27 active images out of 42 distinct images of four-dimensional space-group representations corresponding to points of symmetry. (We warn the reader not to confuse them with the above-mentioned 27 centralizers. The two sets are different.) These active images yield 14 distinct fourth-degree potential types (we will denote them as "FD"). In other words there are 14 centralizers associated with active images and 8 of the 22 centralizers found in Ref. 11 are either Lifshitz inactive or irrelevant to space-group representations. We shall analyze 10 quartic potential types in this paper.

The outline of each section of the present paper is as follows. For each distinct quartic potential type, its centralizer is identified using the notation used in Ref. 12. (In order to avoid excessive digression and confusion, we refer the reader to Ref. 12 for details. Here our intention is to match our notation with that of Ref. 12.) The free energy is expanded to fourth-degree in order-parameter components (to sixth-degree in the case where the fourth-degree expansion is isotropic). The "orbit space"[8] for the potential is depicted and the "phase diagram" is presented. We point out discrepancies with the results of Tolédano and Tolédano,[4] if any. We discuss the degeneracies between phases, the degree at which, in the polynomial expansion, free energies for different images begin to be

 ©1986 The American Physical Society

different, and what needs to be done to lift these degeneracies. We also check whether the Ascher[13] and the Michel-Radicati[14] conjectures on minimal symmetry breaking hold.

II. MATHEMATICAL PRELIMINARIES

For four-dimensional irreducible representations of space groups, Gufan and Sakhnenko[2] stated that there can be at most 24 images satisfying the Liftshitz condition but not necessarily the Landau condition. Tolédano and Tolédano[4] reported 22 active four-dimensional images. We have found 5 additional active images. As a whole we have found[15] 132 distinct images for all space-group representations corresponding to points of symmetry. In our notation for images the first letter stands for dimension (*A* for one dimension, *B* for two, *C* for three, *D* for four, etc.). The second number stands for the order of the image group and the last letter for each different image with the same dimension and order. In Fig. 1 we show group-subgroup relations among all four-dimensional active images. A solid line means a "direct" group-subgroup relation (the set of matrices representing the lower-order group is a subset of that of the higher-order group), and a dashed line means an "indirect" group-subgroup relation (the latter set is not identical to but only equivalent to a subset of the former set).

Any group invariant polynomial $P(\phi_i)$ can be expressed as a polynomial of basic invariant polynomials $D_\alpha(\phi_i)$ and $N_\beta(\phi_i)$ in the form,

$$P(\phi_i)=\sum_\beta q_\beta(D_1,D_2,\ldots,D_n)N_\beta(\phi_i)\ , \tag{1}$$

where $N_1=1$ and $q_\beta(D_1D_2,\ldots,D_n)$ are polynomials of D_α and for some integers ν_β, $(N_\beta)^{\nu_\beta}$ are again polynomials of D_α, but D_α are algebraically independent from each other. See Ref. 3 for some examples. The set of D_α and N_β is called the integrity basis. A polynomial expansion of the free energy truncated at some degree can also be written in the form of Eq. (1).

If Eq. (1) is applied to quartic interaction terms as used in the renormalization-group methods, it yields the familiar equation

$$P(\phi_i)=\sum_\nu u_\nu I_\nu^{(4)}(\phi_i)\ .$$

Since $I_0^{(4)}\equiv I_2^2=(\sum_i\phi_i^2)^2$ is the only polynomial identity that can be formed at fourth degree, the rest of $I_i^{(4)}$'s are fourth-degree basic invariant polynomials. Here

$$q_1(D_1,D_2,\ldots,D_n)=u_0I_2^2+u_1I_1^{(4)}+\cdots$$

is linear in D_α (except that it is quartic in I_2) and

$$q_\beta(D_1,D_2,\ldots,D_n)=1\quad(\beta>1)$$

for some I_ν's identified as N_β's.

Thus it is natural for us to find the basic invariant polynomials D_α's and N_β's for each image before we at-

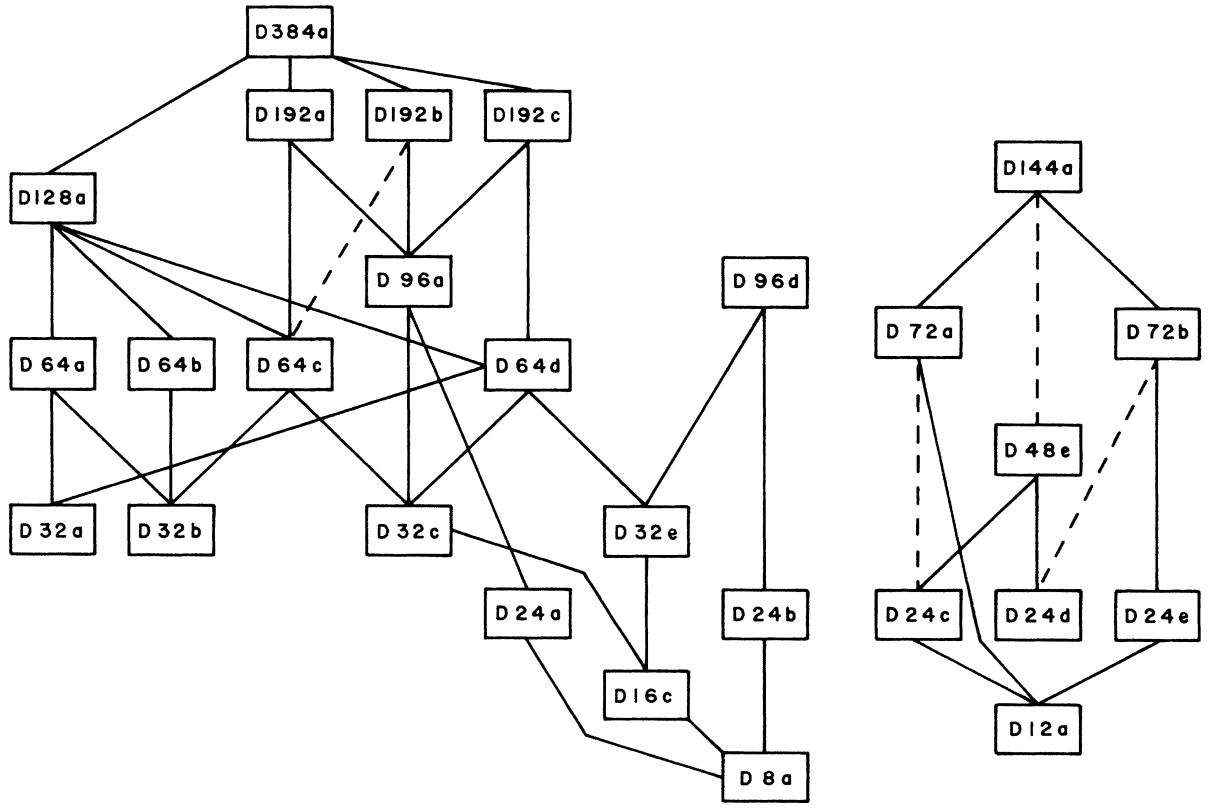

FIG. 1. Group-subgroup trees of active four-dimensional images. Solid lines mean direct inclusion and dotted lines mean indirect inclusion. The notations for images are the same as those of Ref. 15.

TABLE I. Images of active space-group representations and their integrity basis up to the sixth degree. Images with the same fourth-degree integrity basis are grouped together and identified with their centralizers.

Centralizer	Image	Irrep	Space group		Fourth degree	Sixth degree
FD1	$D\,384a$	$L_1^{\pm},L_2^{\pm}$	O_h^7	($Fd3m$; No. 227)	$I_1^{(4)}$	$I_1^{(6)}$
$\left[\frac{O}{D_2};\frac{O}{D_2}\right]^*$	$D\,192a$	$L_1^{\pm}$	T_h^4	($Fd3$; No. 203)	$I_1^{(4)}$	$I_1^{(6)}$
	$D\,192c$	L_1,L_2	O^4	($F4_132$; No. 210)	$I_1^{(4)}$	$I_1^{(6)}$
FD2	$D\,192b$	L_1,L_2	O^3	($F432$; No. 209)	$I_1^{(4)},I_2^{(4)}$	$I_1^{(6)}$
		L_1,L_2	T_d^2	($F\bar{4}3m$; No. 216)		
$\left[\frac{T}{D_2};\frac{T}{D_2}\right]^*$		$L_1^{\pm},L_2^{\pm}$	O_h^5	($Fm3m$; No. 225)		
	$D\,96a$	L_1	T^2	($F23$; No. 196)	$I_1^{(4)},I_2^{(4)}$	$I_1^{(6)}$
		$L_1^{\pm}$	T_h^3	($Fm3$; No. 202)		
FD3	$D\,128a$	$N_1^{\pm},N_2^{\pm}$	D_{4h}^{19}	($I4_1/amd$; No. 141)	$I_1^{(4)},I_3^{(4)}$	$I_1^{(6)}$
	$D\,64a$	$N_1^{\pm}$	C_{4h}^6	($I4_1/a$; No. 88)	$I_1^{(4)},I_3^{(4)}$	$I_1^{(6)},I_2^{(6)}$
$\left[\frac{D_4}{D_2};\frac{D_4}{D_2}\right]^*$		N_1,N_2	C_{4v}^{11}	($I4_1md$; No. 109)		
	$D\,64b$	N_1,N_2	D_{2d}^{12}	($I\bar{4}2d$; No. 122)	$I_1^{(4)},I_3^{(4)}$	$I_1^{(6)}$
	$D\,64d$	N_1,N_2	D_4^{10}	($I4_122$; No. 98)	$I_1^{(4)},I_3^{(4)}$	$I_1^{(6)}$
	$D\,32a$	N_1	C_4^6	($I4_1$; No. 80)	$I_1^{(4)},I_3^{(4)}$	$I_1^{(6)},I_2^{(6)},I_3^{(6)}$
FD4	$D\,64c$	$L_1^{\pm}$	D_{2h}^{24}	($Fddd$; No. 70)	$I_1^{(4)},I_3^{(4)},I_4^{(4)}$	$I_1^{(6)}$
$(D_2\times D_2)^*$		N_1,N_2	D_4^9	($I422$; No. 97)		
		N_1,N_2	C_{4v}^9	($I4mm$; No. 107)		
		N_1,N_2	D_{2d}^9	($I\bar{4}m2$; No. 119)		
		N_1,N_2	D_{2d}^{11}	($I\bar{4}2m$; No. 121)		
		$N_1^{\pm},N_2^{\pm}$	D_{4h}^{17}	($I4/mmm$; No. 139)		
	$D\,32b$	L_1	C_{2v}^{19}	($Fdd2$; No. 43)	$I_1^{(4)},I_3^{(4)},I_4^{(4)}$	$I_1^{(6)},I_2^{(6)}$
		N_1	C_4^5	($I4$; No. 79)		
		N_1	S_4^2	($I\bar{4}$; No. 82)		
		$N_1^{\pm}$	C_{4h}^5	($I4/m$; No. 87)		
		$R_1^{\pm}$	D_{4h}^6	($P4/mnc$; No. 128)		
		$R_1^{\pm}$	D_{4h}^{14}	($P4_2/mnm$; No. 136)		
FD5	$D\,32e$	$R_1\oplus R_3,\ R_2\oplus R_4$	D_4^4	($P4_12_12$; No. 92)	$I_1^{(4)},I_3^{(4)},I_5^{(4)}$	$I_1^{(6)},I_4^{(6)}$
$\left[\frac{C_8}{C_4};\frac{D_4}{D_2}\right]$		$R_1\oplus R_3,\ R_2\oplus R_4$	D_4^8	($P4_32_12$; No. 96)		
FD6	$D\,32c$	L_1	D_2^7	($F222$; No. 22)	$I_1^{(4)},I_2^{(4)},I_3^{(4)},I_4^{(4)}$	$I_1^{(6)}$
$(D_2\times D_2)$		L_1	C_{2v}^{18}	($Fmm2$; No. 42)		
		$L_1^{\pm}$	D_{2h}^{23}	($Fmmm$; No. 69)		

TABLE I. (*Continued*).

Centralizer	Image	Irrep	Space group		Fourth degree	Sixth degree
FD7 $\left[\frac{C_6}{C_2};\frac{T}{D_2}\right]$	$D24a$	$R_1^+\oplus R_3^+, R_1^-\oplus R_3^-$	T_h^6	($Pa3$; No. 205)	$I_1^{(4)}, -I_5^{(4)}+I_7^{(4)}+I_9^{(4)}$ $I_2^{(4)}, I_6^{(4)}+I_8^{(4)}-I_{10}^{(4)}$	$I_1^{(6)}, I_4^{(6)}-I_6^{(6)}-I_8^{(6)},$ $I_5^{(6)}+I_7^{(6)}-I_9^{(6)}$
FD8	$D96d$	$P_1\oplus P_1^*, P_2\oplus P_2^*$	T_d^6	($I\bar{4}3d$; No. 220)	none	$I_{10}^{(6)}, I_{11}^{(6)}$
$O(4)$	$D24b$	$R_2^+\oplus(R_2^+)^*, R_2^-\oplus(R_2^-)^*$	T_h^6	($Pa3$; No. 205)	none	$I_{10}^{(6)}, \ldots, I_{16}^{(6)}$
FD9 $(C_4\times D_2)$	$D16c$	$R_1^+\oplus R_2^+, R_1^-\oplus R_2^-$	D_{2h}^{18}	($Cmca$; No. 64)	$I_1^{(4)}, \ldots, I_6^{(4)}$	$I_1^{(6)}, I_4^{(6)}, I_5^{(6)}$
FD10 $(C_2\times D_2)$	$D8a$	$R_1^+\oplus(R_1^+)^*, R_1^-\oplus(R_1^-)^*$	D_{2h}^{15}	($Pbca$; No. 61)	$I_1^{(4)}, \ldots, I_{10}^{(4)}$	$I_1^{(6)}, I_4^{(6)}, \ldots, I_9^{(6)}$
FD11	$D144a$	H_1, H_2	D_{6h}^4	($P6_3/mmc$; No. 194)	$J_1^{(4)}$	$I_{17}^{(6)}$
$(D_\infty\times D_\infty)^*$	$D72a$	H_3	C_{6v}^4	($P6_3mc$; No. 186)	$J_1^{(4)}$	$I_{17}^{(6)}$
	$D72b$	$H_3\oplus H_6, H_4\oplus H_5$	C_{6h}^2	($P6_3/m$; No. 176)	$J_1^{(4)}$	$I_{17}^{(6)}, I_{18}^{(6)}$
		$H_1\oplus H_1^*, H_2\oplus H_2^*$	D_{3h}^4	($P\bar{6}2c$; No. 190)		
FD12	$D48e$	P_3	O_h^9	($Im3m$; No. 229)	$J_1^{(4)}, J_2^{(4)}$	$I_{21}^{(6)}, I_{23}^{(6)}$
$(D_2\times D_\infty)$	$D24d$	$P_2\oplus P_3$	T_h^5	($Im3$; No. 204)	$J_1^{(4)}, J_2^{(4)}$	$I_{19}^{(6)}, \ldots, I_{23}^{(6)}$
FD13	$D24c$	$P_3\oplus P_3^*$	T_d^3	($I\bar{4}3m$; No. 217)	$J_1^{(4)}, J_2^{(4)}, I_6^{(4)}$	$I_{21}^{(6)}, I_{23}^{(6)}, I_{24}^{(6)}$
$(C_4\times D_\infty)$	$D24e$	$R_2\oplus R_3$	O_h^2	($Pn3n$; No. 222)	$J_1^{(4)}, J_2^{(4)}, I_6^{(4)}$	$I_{17}^{(6)}, I_{18}^{(6)}, I_{25}^{(6)}, I_{26}^{(6)}$
		$R_2\oplus R_3$	O_h^3	($Pm3n$; No. 223)		
		$H_2\oplus H_3$	O_h^{10}	($Ia3d$; No. 230)		
FD14	$D12a$	$R_3\oplus R_3^*$	T_d^4	($P\bar{4}3n$; No. 218)	$J_1^{(4)}, J_2^{(4)}, I_6^{(4)},$	$I_{17}^{(6)}, I_{18}^{(6)}, I_{21}^{(6)},$
$(C_2\times D_\infty)$		$H_3\oplus H_3^*$	T_d^6	($I\bar{4}3d$; No. 220)	$I_7^{(4)}+I_8^{(4)}, I_9^{(4)}+I_{10}^{(4)}$	$I_{25}^{(6)}, \ldots, I_{28}^{(6)}$

TABLE II. Fourth- and sixth-degree basic invariant polynomilas for Table I.

$$I_1^{(4)}=\eta_1^4+\zeta_1^4+\eta_2^4+\zeta_2^4$$
$$I_2^{(4)}=\eta_1\zeta_1\eta_2\zeta_2$$
$$I_3^{(4)}=\eta_1^2\zeta_1^2+\eta_2^2\zeta_2^2$$
$$I_4^{(4)}=\eta_1^2\eta_2^2+\zeta_1^2\zeta_2^2$$
$$I_5^{(4)}=\eta_1\zeta_1(\eta_1^2-\zeta_1^2)-\eta_2\zeta_2(\eta_2^2-\zeta_2^2)$$
$$I_6^{(4)}=\eta_1\zeta_1(\eta_2^2-\zeta_2^2)-\eta_2\zeta_2(\eta_1^2-\zeta_1^2)$$
$$I_7^{(4)}=\eta_1\eta_2(\eta_1^2-\eta_2^2)+\zeta_1\zeta_2(\zeta_1^2-\zeta_2^2)$$
$$I_8^{(4)}=\eta_1\eta_2(\zeta_1^2-\zeta_2^2)+\zeta_1\zeta_2(\eta_1^2-\eta_2^2)$$
$$I_9^{(4)}=\eta_1\zeta_2(\eta_1^2-\zeta_2^2)-\zeta_1\eta_2(\zeta_1^2-\eta_2^2)$$
$$I_{10}^{(4)}=\eta_1\zeta_2(\zeta_1^2-\eta_2^2)-\zeta_1\eta_2(\eta_1^2-\zeta_2^2)$$
$$J_1^{(4)}=I_1^{(4)}+2I_3^{(4)}$$
$$J_2^{(4)}=I_4^{(4)}+2I_2^{(4)}$$
$$I_1^{(6)}=\eta_1^6+\zeta_1^6+\eta_2^6+\zeta_2^6$$
$$I_2^{(6)}=\eta_1\zeta_1\eta_2\zeta_2(\eta_1^2+\zeta_1^2-\eta_2^2-\zeta_2^2)$$
$$I_3^{(6)}=\eta_1^4\eta_2^2+\eta_1^2\zeta_2^4+\zeta_1^4\zeta_2^2+\zeta_1^2\eta_2^4$$
$$I_4^{(6)}=\eta_1\zeta_1(\eta_1^4-\zeta_1^4)-\eta_2\zeta_2(\eta_2^4-\zeta_2^4)$$
$$I_5^{(6)}=\eta_1\zeta_1(\eta_2^4-\zeta_2^4)-\eta_2\zeta_2(\eta_1^4-\zeta_1^4)$$
$$I_6^{(6)}=\eta_1\eta_2(\eta_1^4-\eta_2^4)+\zeta_1\zeta_2(\zeta_1^4-\zeta_2^4)$$
$$I_7^{(6)}=\eta_1\eta_2(\zeta_1^4-\zeta_2^4)+\zeta_1\zeta_2(\eta_1^4-\eta_2^4)$$
$$I_8^{(6)}=\eta_1\zeta_2(\eta_1^4-\zeta_2^4)-\zeta_1\eta_2(\zeta_1^4-\eta_2^4)$$
$$I_9^{(6)}=\eta_1\zeta_2(\zeta_1^4-\eta_2^4)-\zeta_1\eta_2(\eta_1^4-\zeta_2^4)$$
$$I_{10}^{(6)}=3(\eta_1^6+\zeta_1^6+\eta_2^6+\zeta_2^6)+5(\eta_1^4+\zeta_1^4+6\eta_1^2\zeta_1^2)(\eta_2^2+\zeta_2^2)$$
$$+5(\eta_2^4+\zeta_2^4+6\eta_2^2\zeta_2^2)(\eta_1^2+\zeta_1^2)+5\eta_1^2\zeta_1^2(\eta_1^2+\zeta_1^2)+5\eta_2^2\zeta_2^2(\eta_2^2+\zeta_2^2)$$
$$I_{11}^{(6)}=\eta_1\zeta_1[(\eta_1^4-\zeta_1^4)-5(\eta_1^2-\zeta_1^2)(\eta_2^2+\zeta_2^2)]-\eta_2\zeta_2[(\eta_2^4-\zeta_2^4)-5(\eta_2^2-\zeta_2^2)(\eta_1^2+\zeta_1^2)]$$
$$I_{12}^{(6)}=\eta_1\eta_2[(\eta_1^4-\eta_2^4)-5(\eta_1^2-\eta_2^2)(\zeta_1^2+\zeta_2^2)]+\zeta_1\zeta_2[(\zeta_1^4-\zeta_2^4)-5(\zeta_1^2-\zeta_2^2)(\eta_1^2+\eta_2^2)]$$
$$I_{13}^{(6)}=\eta_1\zeta_2[(\eta_1^4-\zeta_2^4)-5(\eta_1^2-\zeta_2^2)(\eta_2^2+\zeta_1^2)]+\eta_2\zeta_1[(\eta_2^4-\zeta_1^4)-5(\eta_2^2-\zeta_1^2)(\eta_1^2+\zeta_2^2)]$$
$$I_{14}^{(6)}=\eta_1\zeta_1[(\eta_2^4-\zeta_2^4)-(\eta_2^2-\zeta_2^2)(\eta_1^2+\zeta_1^2)]-\eta_2\zeta_2[(\eta_1^4-\zeta_1^4)-(\eta_1^2-\zeta_1^2)(\eta_2^2+\zeta_2^2)]$$
$$I_{15}^{(6)}=\eta_1\eta_2[(\zeta_1^4-\zeta_2^4)-(\zeta_1^2-\zeta_2^2)(\eta_1^2+\eta_2^2)]+\zeta_1\zeta_2[(\eta_1^4-\eta_2^4)-(\eta_1^2-\eta_2^2)(\zeta_1^2+\zeta_2^2)]$$
$$I_{16}^{(6)}=\eta_1\zeta_2[(\eta_2^4-\zeta_1^4)-(\eta_2^2-\zeta_1^2)(\eta_1^2+\zeta_2^2)]+\eta_2\zeta_1[(\eta_1^4-\zeta_2^4)-(\eta_1^2-\zeta_2^2)(\eta_2^2+\zeta_1^2)]$$
$$I_{17}^{(6)}=11\eta_1^6+15\eta_1^4\zeta_1^2+45\eta_1^2\zeta_1^4+9\zeta_1^6+11\eta_2^6+15\eta_2^4\zeta_2^2+45\eta_2^2\zeta_2^4+9\zeta_2^6$$
$$I_{18}^{(6)}=\eta_1\zeta_1[3(\eta_1^4+\zeta_1^4)-10\eta_1^2\zeta_1^2]-\eta_2\zeta_2[3(\eta_2^4+\zeta_2^4)-10\eta_2^2\zeta_2^2]$$
$$I_{19}^{(6)}=\eta_1\zeta_1[(\eta_2^4-\zeta_2^4)-(\eta_1^2+\zeta_1^2)(\eta_2^2-\zeta_2^2)]+\eta_2\zeta_2[(\eta_1^4-\zeta_1^4)-(\eta_2^2+\zeta_2^2)(\eta_1^2-\zeta_1^2)]$$
$$I_{20}^{(6)}=\eta_1\eta_2[3(\eta_1^2\zeta_2^2+\zeta_1^2\eta_2^2)-\eta_1^2\eta_2^2-9\zeta_1^2\zeta_2^2]-\zeta_1\zeta_2[3(\eta_1^2\zeta_2^2+\zeta_1^2\eta_2^2)-\zeta_1^2\zeta_2^2-9\eta_1^2\eta_2^2]$$
$$I_{21}^{(6)}=\eta_1\zeta_2[3(\eta_1^2\eta_2^2+\zeta_1^2\zeta_2^2)-\eta_1^2\zeta_2^2-9\zeta_1^2\eta_2^2]+\zeta_1\eta_2[3(\eta_1^2\eta_2^2+\zeta_1^2\zeta_2^2)-\zeta_1^2\eta_2^2-9\eta_1^2\zeta_2^2]$$
$$I_{22}^{(6)}=\eta_1\eta_2[(\eta_1^4+\eta_2^4)+5(\zeta_1^4+\zeta_2^4)-10(\eta_1^2\zeta_1^2+\eta_2^2\zeta_2^2)]-\zeta_1\zeta_2[(\zeta_1^4+\zeta_2^4)+5(\eta_1^4+\eta_2^4)-10(\eta_1^2\zeta_1^2+\eta_2^2\zeta_2^2)]$$
$$I_{23}^{(6)}=\eta_1\zeta_2[(\eta_1^4+\zeta_2^4)+5(\zeta_1^4+\eta_2^4)-10(\eta_1^2\zeta_1^2+\eta_2^2\zeta_2^2)]+\zeta_1\eta_2[(\zeta_1^4+\eta_2^4)+5(\eta_1^4+\zeta_2^4)-10(\eta_1^2\zeta_1^2+\eta_2^2\zeta_2^2)]$$
$$I_{24}^{(6)}=\eta_1\eta_2[(\eta_1^4-\eta_2^4)+5(\zeta_1^4-\zeta_2^4)-10(\eta_1^2\zeta_1^2-\eta_2^2\zeta_2^2)]-\zeta_1\zeta_2[(\zeta_1^4-\zeta_2^4)+5(\eta_1^4-\eta_2^4)-10(\eta_1^2\zeta_1^2-\eta_2^2\zeta_2^2)]$$
$$I_{25}^{(6)}=11\eta_1^2\eta_2^2(\eta_1^2+\eta_2^2)+\eta_1^2\zeta_2^2(\eta_1^2+3\zeta_2^2)+\zeta_1^2\eta_2^2(\eta_2^2+3\zeta_1^2)+9\zeta_1^2\zeta_2^2(\zeta_1^2+\zeta_2^2)$$
$$+6\eta_1^2\zeta_1^2(\eta_2^2+3\zeta_2^2)+6\eta_2^2\zeta_2^2(\eta_1^2+3\zeta_1^2)+\eta_1\zeta_1\eta_2\zeta_2(8\eta_1^2+24\zeta_1^2+8\eta_2^2+24\zeta_2^2)$$
$$I_{26}^{(6)}=\eta_1\zeta_1[(5\eta_2^4-3\zeta_2^4)+(\eta_2^2-\zeta_2^2)(2\eta_1^2+6\zeta_1^2)-6\eta_2^2\zeta_2^2]-\eta_2\zeta_2[(5\eta_1^4-3\zeta_1^4)+(\eta_1^2-\zeta_1^2)(2\eta_2^2+6\zeta_2^2)-6\eta_1^2\zeta_1^2]$$
$$I_{27}^{(6)}=\eta_1\eta_2[11(\eta_1^4-\eta_2^4)+15(\zeta_1^4-\zeta_2^4)+10(\eta_1^2\zeta_1^2-\eta_2^2\zeta_2^2)]+\zeta_1\zeta_2[9(\zeta_1^4-\zeta_2^4)+5(\eta_1^4-\eta_2^4)+30(\eta_1^2\zeta_1^2-\eta_2^2\zeta_2^2)]$$
$$I_{28}^{(6)}=\eta_1\zeta_2[11\eta_1^4-9\zeta_2^4+15\zeta_1^4-5\eta_2^4-30\eta_2^2\zeta_2^2+10\eta_1^2\zeta_1^2]+\zeta_1\eta_2[11\eta_2^4-9\zeta_1^4+15\zeta_2^4-5\eta_1^4-30\eta_1^2\zeta_1^2+10\eta_2^2\zeta_2^2]$$

tempt to write the Landau potential. Though in some cases there is no unique way to separate D_α's from N_β's, we can in any case choose a set $\{D_1, D_2, \ldots, D_n\}$ such that they are algebraically independent. In Table I we list space-group representations and the fourth- and sixth-degree basic invariant polynomials for each four-dimensional active image. We use the international symbols[16] for space groups and those of Ref. 6 for representations. In Table II we list specific forms of the basic invariant polynomials, and in Table III we list the number of linearly independent (but not necessarily basic) invariant polynomials at each degree up to the sixteenth-degree for each active image.

When the vector representations, whose transforming matrices are the matrices of the image itself (in this sense we can unambiguously call the vector representation the image), of an image group and its subgroup have the same number of invariant polynomials at each degree up to a

certain degree, their invariant polynomials are identical up to that degree. In this case the free energies for different images are identical up to that degree. Thus Table III and Fig. 1 are very useful in determining the degree to which the free energy should be expanded to distinguish images.

The Landau potential expanded up to the fourth-degree in the order-parameter components ϕ_i can be written in the following generic form:

$$G(\phi_i)=\frac{a}{2}I_2(\phi_i)+\tfrac{1}{4}\left[A_0 I_2^2(\phi_i)+\sum_{\alpha=1}^{\nu} A_\alpha I_\alpha^{(4)}(\phi_i)\right]$$

$$=\frac{a}{2}\eta^2+\tfrac{1}{4}\eta^4(A_0+A_1\lambda_1+A_2\lambda_2+\cdots)\,, \tag{2}$$

where $\eta^2\equiv I_2(\phi_i)=\phi_1^2+\phi_2^2+\phi_3^2+\phi_4^2$, $I_\alpha^{(4)}(\phi_i)$ are linearly independent fourth-degree invariant polynomials, and $\lambda_\alpha\equiv I_\alpha^{(4)}/I_2^2$. The coupling constants $(a,A_0,A_1,\cdots)$ carry pressure and temperature dependence of the free energy. As we go across the transition temperature, a changes sign. The positivity condition,

$$A_0+A_1\lambda_1+A_2\lambda_2+\cdots>0\,, \tag{3}$$

is assumed as usual. The directional minimum along a direction specified by $(\lambda_1,\lambda_2,\cdots)$ is given by

$$\eta_0^2=-\frac{a}{A_0+A_1\lambda_1+A_2\lambda_2+\cdots}\,, \tag{4}$$

$$G_0(\lambda_1,\lambda_2,\cdots)=-\frac{1}{4}\frac{a^2}{A_0+A_1\lambda_1+A_2\lambda_2+\cdots}\,. \tag{5}$$

The absolute minimum is located at η_0 in the direction where $G_0(\lambda_1,\lambda_2,\cdots)$ takes the minimum value or where $A_0+A_1\lambda_1+A_2\lambda_2+\cdots$ is minimized. The points $(\lambda_1,\lambda_2,\ldots)$ occupy a localized region called the orbit space.[17] The absolute minimum is found at the point on the orbit space boundary where the contour

$$A_0+A_1\lambda_1+A_2\lambda_2+\cdots=k \tag{6}$$

moving from $k=0$ to $k=\infty$ makes the first contact. When the orbit space is higher than three-dimensional it is hard to visualize this procedure geometrically. We project the orbit space further onto a two-dimensional plane. The projection depends on the coupling constants A_i's. Thus we shall frequently use a two-dimensional contour

$$A_x\lambda_x+A_y\lambda_y=k\,. \tag{7}$$

Its slope and moving direction as k increases from 0 is shown in Fig. 2 for each pair of signs of A_x and A_y.

Once we build the orbit space relevant to a quartic potential, the phase diagram can be obtained readily. The simplest but not the most efficient way to build the orbit space is to give random values for the order-parameter components. A more efficient way is to anticipate the orbit space boundary using some known properties of the orbit space. The vector space ϕ_i $(i=1,\ldots,n)$ consists of disjoint orbits. We have tabulated orbit structures for the four-dimensional active images in Table IV. (We remind the reader that for a given orbit representative there are a number of equivalent vectors yielding the same numerical values for all group invariant functions.) It is known[18]

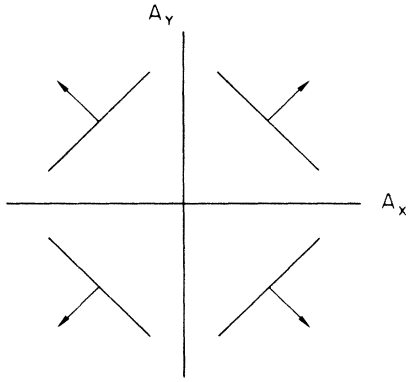

FIG. 2. Slope and movement of the contour $A_x\lambda_x+A_y\lambda_y=k$ as k increases from 0 to $+\infty$, shown for each pair of signs of A_x and A_y.

that low-dimensional orbits corresponding to isotropy subgroups of lower indices tend to form the orbit space boundary. However, there are cases where portions of the boundary are made of high-dimensional orbits. In such cases we need to solve the boundary conditions (see Ref. 8) to find those portions.

It is therefore important to find the orbit structure for each image. In order to achieve this we first find the isotropy subgroups using the subduction criterion,[19] identify those matrices $\Gamma(g_\alpha)$ belonging to a particular isotropy subgroup H also, and then solve a set of linear equations $\Gamma(g_\alpha)\phi=\phi$, $(g_\alpha\in H)$ to find the orbit representative. In Table V we list "orbit parameters" for one-dimensional orbits, which occur frequently in the text.

III. FD1—$(O/D_2;O/D_2)^*$: IMAGES $D384a$, $D192a$, $D192c$

The free energy up to the fourth-degree is given by

$$G=\frac{a}{2}I_2+\tfrac{1}{4}(A_0 I_2^2+A_1 I_1^{(4)})\,. \tag{8}$$

The orbit space is depicted in Fig. 3. The stable phases are listed in Table VI.

Only two phases, $P1$ and $P11$, can be realized at fourth degree. It takes a sixth-degree expansion to realize $P3$ and $P10$. [Up to the sixth-degree the integrity basis is the same as that of the adjoint representation of SO(9), see Ref. 10.]

The three images $D384a$, $D192a$, and $D192c$ are identical up to the tenth degree as can be seen in Table III. The image $D192a$ begins to be different from others at twelfth degree and the other two can be distinguished only at sixteenth degree. Since both $P1$ and $P11$ correspond to maximal isotropy subgroups for each image, neither the Ascher nor the Michel-Radicati conjecture is violated.

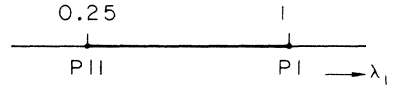

FIG. 3. Orbit space λ_1 for FD1.

TABLE III. The number of linearly independent invariant polynomials at each degree for each image.

FD	Image	2	4	6	8	10	12	14	16
FD1	*D*384*a*	1	2	3	5	6	9	11	15
	*D*192*a*	1	2	3	5	6	10	12	17
	*D*192*c*	1	2	3	5	6	9	11	16
FD2	*D*192*b*	1	3	4	7	9	14	17	24
	*D*96*a*	1	3	4	7	9	15	18	27
FD3	*D*128*a*	1	3	4	8	10	16	20	29
	*D*64*a*	1	3	5	10	14	22	30	43
	*D*64*b*	1	3	4	8	11	18	24	35
	*D*64*d*	1	3	4	9	11	19	24	37
	*D*32*a*	1	3	6	13	19	31	44	65
FD4	*D*64*c*	1	4	5	11	14	24	30	45
	*D*32*b*	1	4	6	13	19	32	44	65
FD5	*D*32*e*	1	4	6	14	19	33	44	67
FD6	*D*32*c*	1	5	6	15	19	35	44	69
FD7	*D*24*a*	1	5	8	17	25	43	58	87
FD8	*D*96*d*	1	1	3	6	6	13	17	22
	*D*24*b*	1	1	8	17	17	43	58	75
FD9	*D*16*c*	1	7	10	25	35	63	84	129
FD10	*D*8*a*	1	11	18	45	67	119	164	249
FD11	*D*144*a*	1	2	3	5	6	11	13	18
	*D*72*a*	1	2	3	7	8	17	21	30
	*D*72*b*	1	2	4	7	9	17	22	30
FD12	*D*48*e*	1	3	5	10	13	24	31	45
	*D*24*d*	1	3	8	15	23	41	58	81
FD13	*D*24*c*	1	4	7	17	22	43	57	84
	*D*24*e*	1	4	8	17	23	43	58	84
FD14	*D*12*a*	1	6	13	31	42	81	111	162

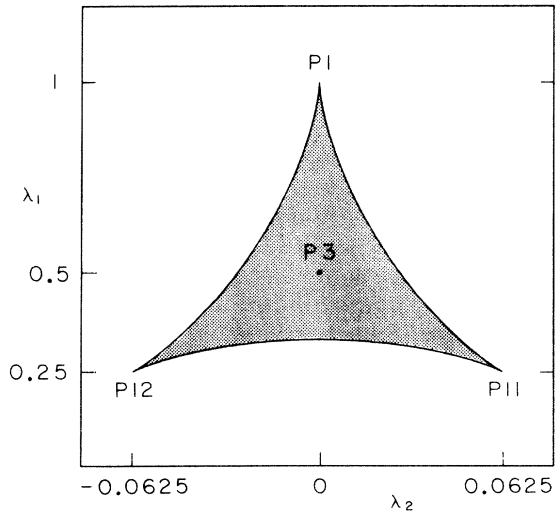

FIG. 4. Orbit space (λ_1,λ_2) for FD2.

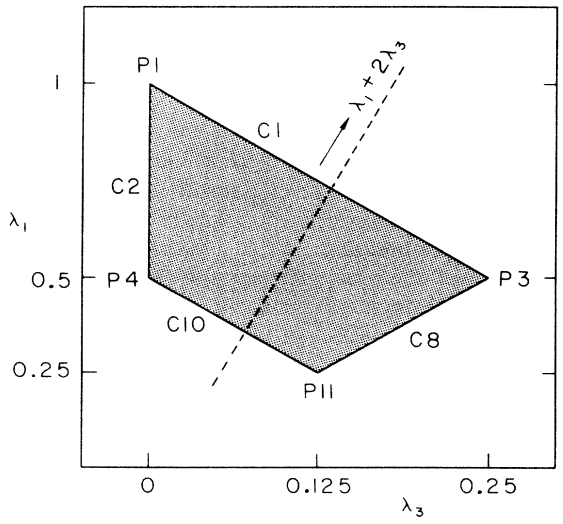

FIG. 5. Orbit space (λ_1,λ_3) for FD3.

TABLE IV. The entire orbit structure of each image. The orbits of maximal isotropy subgroups are marked with asterisks.

Image	Orbit	Invariant vector				Image	Orbit	Invariant vector			
*D*384*a*	*P*1*	*a*	0	0	0	*D*192*c*	*P*1*	*a*	0	0	0
	*P*3*	*a*	*a*	0	0		*P*3*	*a*	*a*	0	0
	*P*10*	*a*	*a*	*a*	0		*P*10*	*a*	*a*	*a*	0
	*P*11*	*a*	*a*	*a*	*a*		*P*11*	*a*	*a*	*a*	*a*
	*C*1	*a*	*b*	0	0		*C*1	*a*	*b*	0	0
	*C*5	*a*	*a*	*b*	0		*C*5	*a*	*a*	*b*	0
	*C*7	*a*	*a*	*a*	*b*		*C*7	*a*	*a*	*a*	*b*
	*C*8	*a*	*a*	*b*	*b*		*C*8	*a*	*a*	*b*	*b*
	*S*1	*a*	*b*	*c*	0		4*D*1	*a*	*b*	*c*	*d*
	*S*2	*a*	*a*	*b*	*c*						
	4*D*1	*a*	*b*	*c*	*d*						
*D*192*a*	*P*1*	*a*	0	0	0						
	*P*3*	*a*	*a*	0	0						
	*P*10*	*a*	*a*	*a*	0						
	*P*11*	*a*	*a*	*a*	*a*						
	*C*1	*a*	*b*	0	0						
	*C*7	*a*	*a*	*a*	*b*						
	*C*8	*a*	*a*	*b*	*b*						
	*S*1	*a*	*b*	*c*	0						
	4*D*1	*a*	*b*	*c*	*d*						
*D*192*b*	*P*1*	*a*	0	0	0	*D*96*a*	*P*1*	*a*	0	0	0
	*P*3*	*a*	*a*	0	0		*P*3*	*a*	*a*	0	0
	*P*11*	*a*	*a*	*a*	*a*		*P*11*	*a*	*a*	*a*	*a*
	*P*12*	*a*	*a*	*a*	$-a$		*P*12*	*a*	*a*	*a*	$-a$
	*C*1	*a*	*b*	0	0		*C*1	*a*	*b*	0	0
	*C*7	*a*	*a*	*a*	*b*		*C*7	*a*	*a*	*a*	*b*
	*C*8	*a*	*a*	*b*	*b*		*C*8	*a*	*a*	*b*	*b*
	*C*9	*a*	*a*	*b*	$-b$		*C*9	*a*	*a*	*b*	$-b$
	*S*2	*a*	*a*	*b*	*c*		4*D*1	*a*	*b*	*c*	*d*
	4*D*1	*a*	*b*	*c*	*d*						
*D*64*c*	*P*1*	*a*	0	0	0	*D*32*b*	*P*1*	*a*	0	0	0
	*P*3*	*a*	*a*	0	0		*P*3*	*a*	*a*	0	0
	*P*4*	*a*	0	*a*	0		*P*4*	*a*	0	*a*	0
	*P*5*	*a*	0	0	*a*		*P*5*	*a*	0	0	*a*
	*P*11*	*a*	*a*	*a*	*a*		*C*1	*a*	*b*	0	0
	*C*1	*a*	*b*	0	0		*C*2	*a*	0	*b*	0
	*C*2	*a*	0	*b*	0		*C*3	*a*	0	0	*b*
	*C*3	*a*	0	0	*b*		*C*8	*a*	*a*	*b*	*b*
	*C*8	*a*	*a*	*b*	*b*		4*D*1	*a*	*b*	*c*	*d*
	*C*10	*a*	*b*	*a*	*b*						
	*C*12	*a*	*b*	*b*	*a*						
	*S*1	*a*	*b*	*c*	0						
	4*D*1	*a*	*b*	*c*	*d*						
*D*128*a*	*P*1*	*a*	0	0	0	*D*64*a*	*P*1*	*a*	0	0	0
	*P*3*	*a*	*a*	0	0		*P*3*	*a*	*a*	0	0
	*P*4*	*a*	0	*a*	0		*P*4*	*a*	0	*a*	0
	*P*11*	*a*	*a*	*a*	*a*		*C*1	*a*	*b*	0	0
	*C*1	*a*	*b*	0	0		*C*2	*a*	0	*b*	0
	*C*2	*a*	0	*b*	0		*C*8	*a*	*a*	*b*	*b*
	*C*5	*a*	*a*	*b*	0		*S*2	*a*	*a*	*b*	*c*
	*C*8	*a*	*a*	*b*	*b*		4*D*1	*a*	*b*	*c*	*d*
	*C*10	*a*	*b*	*a*	*b*						
	*S*1	*a*	*b*	*c*	0	*D*64*b*	*P*1*	*a*	0	0	0
	*S*2	*a*	*a*	*b*	*c*		*P*3*	*a*	*a*	0	0
	4*D*1	*a*	*b*	*c*	*d*		*P*4*	*a*	0	*a*	0
							*P*11*	*a*	*a*	*a*	*a*

TABLE IV. (*Continued*).

Image	Orbit	Invariant vector				Image	Orbit	Invariant vector			
*D*64*d*	*P*1*	*a*	0	0	0		*C*1	*a*	*b*	0	0
	*P*3*	*a*	*a*	0	0		*C*2	*a*	0	*b*	0
	*P*4*	*a*	0	*a*	0		*C*5	*a*	*a*	*b*	0
	*P*11*	*a*	*a*	*a*	*a*		*C*8	*a*	*a*	*b*	*b*
	*C*1	*a*	*b*	0	0		4*D*1	*a*	*b*	*c*	*d*
	*C*2	*a*	0	*b*	0						
	*C*5	*a*	*a*	*b*	0	*D*32*a*	*P*1*	*a*	0	0	0
	*C*8	*a*	*a*	*b*	*b*		*P*3*	*a*	*a*	0	0
	*C*10	*a*	*b*	*a*	*b*		*C*1	*a*	*b*	0	0
	*C*11	*a*	*b*	*a*	$-b$		*C*2	*a*	0	*b*	0
	4*D*1	*a*	*b*	*c*	*d*		*C*8	*a*	*a*	*b*	*b*
							4*D*1	*a*	*b*	*c*	*d*
*D*32*c*	*P*1*	*a*	0	0	0	*D*32*e*	*C*1*	*a*	*b*	0	0
	*P*3*	*a*	*a*	0	0		*C*11*	*a*	*b*	*a*	$-b$
	*P*4*	*a*	0	*a*	0		4*D*1	*a*	*b*	*c*	*d*
	*P*5*	*a*	0	0	*a*						
	*P*11*	*a*	*a*	*a*	*a*	*D*24*a*	*C*7*	*a*	*a*	*a*	*b*
	*P*12*	*a*	*a*	*a*	$-a$		4*D*1	*a*	*b*	*c*	*d*
	*C*1	*a*	*b*	0	0						
	*C*2	*a*	0	*b*	0	*D*96*d*	*C*1*	*a*	*b*	0	0
	*C*3	*a*	0	0	*b*		4*D*1	*a*	*b*	*c*	*d*
	*C*8	*a*	*a*	*b*	*b*						
	*C*9	*a*	*a*	*b*	$-b$	*D*24*b*	4*D*1*	*a*	*b*	*c*	*d*
	*C*10	*a*	*b*	*a*	*b*						
	*C*11	*a*	*b*	*a*	$-b$	*D*16*c*	*C*1*	*a*	*b*	0	0
	*C*12	*a*	*b*	*b*	*a*		*C*11*	*a*	*b*	*a*	$-b$
	*C*13	*a*	*b*	$-b$	*a*		*C*12*	*a*	*b*	*b*	*a*
	4*D*1	*a*	*b*	*c*	*d*		4*D*1	*a*	*b*	*c*	*d*
						*D*8*a*	4*D*1*	*a*	*b*	*c*	*d*
*D*144*a*	*P*1*	*a*	0	0	0	*D*72*a*	*P*1*	*a*	0	0	0
	*P*2*	0	*a*	0	0		*P*2*	0	*a*	0	0
	*P*4*	*a*	0	*a*	0		*C*1	*a*	*b*	0	0
	*P*8*	0	*a*	0	*a*		*C*2	*a*	0	*b*	0
	*C*1	*a*	*b*	0	0		*C*4	0	*a*	0	*b*
	*C*2	*a*	0	*b*	0		4*D*1	*a*	*b*	*c*	*d*
	*C*3	*a*	0	0	*b*						
	*C*4	0	*a*	0	*b*	*D*72*b*	*C*1*	*a*	*b*	0	0
	*C*10	*a*	*b*	*a*	*b*		*C*11*	*a*	*b*	*a*	$-b$
	*C*11	*a*	*b*	*a*	$-b$		4*D*1	*a*	*b*	*c*	*d*
	4*D*1	*a*	*b*	*c*	*d*						
*D*48*e*	*P*5*	*a*	0	0	*a*	*D*24*c*	*C*12*	*a*	*b*	*b*	*a*
	*P*6*	*a*	0	0	$-a$		*C*14*	*a*	*b*	$-b$	$-a$
	*P*11*	*a*	*a*	*a*	*a*		4*D*1	*a*	*b*	*c*	*d*
	*P*13*	*a*	*a*	$-a$	$-a$						
	*C*3	*a*	0	0	*b*	*D*24*e*	*C*1*	*a*	*b*	0	0
	*C*8	*a*	*a*	*b*	*b*		*C*11*	*a*	*b*	*a*	$-b$
	*C*10	*a*	*b*	*a*	*b*		4*D*1	*a*	*b*	*c*	*d*
	*C*12	*a*	*b*	*b*	*a*						
	*C*13	*a*	*b*	$-b$	*a*	*D*12*a*	4*D*1*	*a*	*b*	*c*	*d*
	*C*14	*a*	*b*	$-b$	$-a$						
	4*D*1	*a*	*b*	*c*	*d*						
*D*24*d*	*C*10*	*a*	*b*	*a*	*b*						
	*C*13*	*a*	*b*	$-b$	*a*						
	4*D*1	*a*	*b*	*c*	*d*						

TABLE V. Orbit parameters (Ref. 8) for one-dimensional orbits occurring frequently in the text.

Phases	Invariant vector	λ_1	λ_2	λ_3	λ_4	λ_5	λ_6
$P1$	$a\ 0\ 0\ 0$	1	0	0	0	0	0
$P2$	$0\ a\ 0\ 0$	1	0	0	0	0	0
$P3$	$a\ a\ 0\ 0$	$\frac{1}{2}$	0	$\frac{1}{4}$	0	0	0
$P4$	$a\ 0\ a\ 0$	$\frac{1}{2}$	0	0	$\frac{1}{4}$	0	0
$P5$	$a\ 0\ 0\ a$	$\frac{1}{2}$	0	0	0	0	0
$P6$	$a\ 0\ 0\ -a$	$\frac{1}{2}$	0	0	0	0	0
$P7$	$a\ 0\ -a\ 0$	$\frac{1}{2}$	0	0	$\frac{1}{4}$	0	0
$P8$	$0\ a\ 0\ a$	$\frac{1}{2}$	0	0	$\frac{1}{4}$	0	0
$P9$	$0\ a\ 0\ -a$	$\frac{1}{2}$	0	0	$\frac{1}{4}$	0	0
$P10$	$a\ a\ a\ 0$	$\frac{1}{3}$	0	$\frac{1}{9}$	$\frac{1}{9}$	0	$\frac{1}{9}$
$P11$	$a\ a\ a\ a$	$\frac{1}{4}$	$\frac{1}{16}$	$\frac{1}{8}$	$\frac{1}{8}$	0	0
$P12$	$a\ a\ a\ -a$	$\frac{1}{4}$	$-\frac{1}{16}$	$\frac{1}{8}$	$\frac{1}{8}$	0	0
$P13$	$a\ a\ -a\ -a$	$\frac{1}{4}$	$\frac{1}{16}$	$\frac{1}{8}$	$\frac{1}{8}$	0	0

TABLE VI. "Phase diagram" for FD1.

Region	Phase
$A_1>0$	$P11$
$A_1<0$	$P1$

TABLE VII. "Phase diagram" for FD2.

Quadrant	Phase	Region
$A_1>0,\ A_2>0$	$P12$	everywhere
$A_1>0,\ A_2<0$	$P11$	everywhere
$A_1<0,\ A_2>0$	$P1$	$12A_1+A_2<0$
	$P12$	$12A_1+A_2>0$
$A_1<0,\ A_2<0$	$P1$	$-12A_1+A_2>0$
	$P11$	$-12A_1+A_2<0$

TABLE VIII. "Phase diagram" for FD3.

Quadrant	Phase	Region
$A_1>0,\ A_3>0$	$P4$	$-2A_1+A_3>0$
	$P11$	$-2A_1+A_3<0$
$A_1>0,\ A_3<0$	$P3$	$2A_1+A_3<0$
	$P11$	$2A_1+A_3>0$
$A_1<0,\ A_3>0$	$P1$	everywhere
$A_1<0,\ A_3<0$	$P1$	$-2A_1+A_3>0$
	$P3$	$-2A_1+A_3<0$

IV. FD2—$(T/D_2;T/D_2)^*$: IMAGES $D192b$ AND $D96a$

The free energy up to the fourth-degree is given by

$$G=\frac{a}{2}I_2+\tfrac{1}{4}(A_0I_2^2+A_1I_1^{(4)}+A_2I_2^{(4)})\ . \tag{9}$$

The orbit space is depicted in Fig. 4. The stable phases are listed in Table VII. The phase $P3$ is not realized at this stage but can be realized at the sixth-degree. [Up to the sixth-degree the integrity basis is the same as that of the adjoint of SO(8).]

TABLE IX. "Phase diagram" for FD4.

Octant		Phase	Region
$A_1>0,\ A_{3,4}>0$	$0°<\theta<90°$	$P5$	$-2A_1+A_3+A_4>0$
		$P11$	$-2A_1+A_3+A_4<0$
	$90°<\theta<180°$	$P3$	$-2A_1-A_3+A_4>0$
		$P11$	$-2A_1-A_3+A_4<0$
$A_1>0,\ A_{3,4}<0$	$0°<\theta<45°$	$P3$	$-2A_1-A_3+A_4>0$
		$P11$	$-2A_1-A_3+A_4<0$
	$45°<\theta<180°$	$P4$	$-2A_1+A_3-A_4>0$
		$P11$	$-2A_1+A_3-A_4<0$
$A_1<0,\ A_{3,4}>0$	$0°<\theta<90°$	$P1$	everywhere
	$90°<\theta<180°$	$P1$	$-2A_1+A_3>0$
		$P3$	$-2A_1+A_3<0$
$A_1<0,\ A_{3,4}<0$	$0°<\theta<45°$	$P1$	$-2A_1+A_3>0$
		$P3$	$-2A_1+A_3<0$
	$45°<\theta<180°$	$P1$	$-2A_1+A_4>0$
		$P4$	$-2A_1+A_4<0$

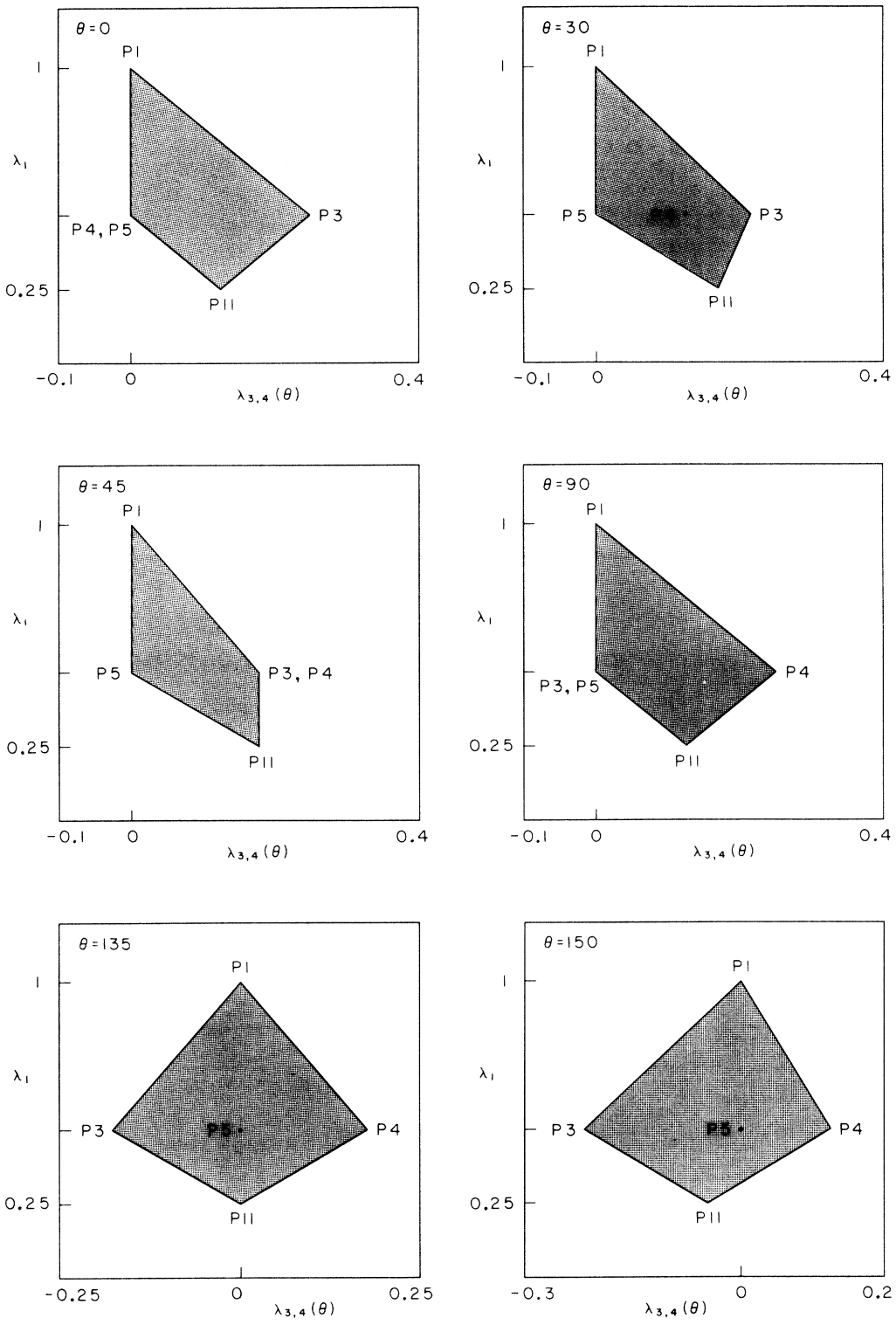

FIG. 6. Orbit space $(\lambda_1, \lambda_3\cos\theta+\lambda_4\sin\theta)$ for FD4.

A twelfth-degree expansion is needed to distinguish $D192b$ from $D96a$. Neither conjecture is violated.

V. FD3—$(D_4/D_2;D_4/D_2)^*$: IMAGES $D128a$, $D64a$, $D64b$, $D64d$, AND $D32a$

The free energy up to the fourth-degree is given by

$$G=\frac{a}{2}I_2+\tfrac{1}{4}(A_0I_2^2+A_1I_1^{(4)}+A_3I_3^{(4)})\,. \tag{10}$$

The orbit space is depicted in Fig. 5. The stable phases are listed in Table VIII.

Images $D64a$ and $D32a$ are distinguished at the sixth degree. An eighth-degree expansion distinguishes image

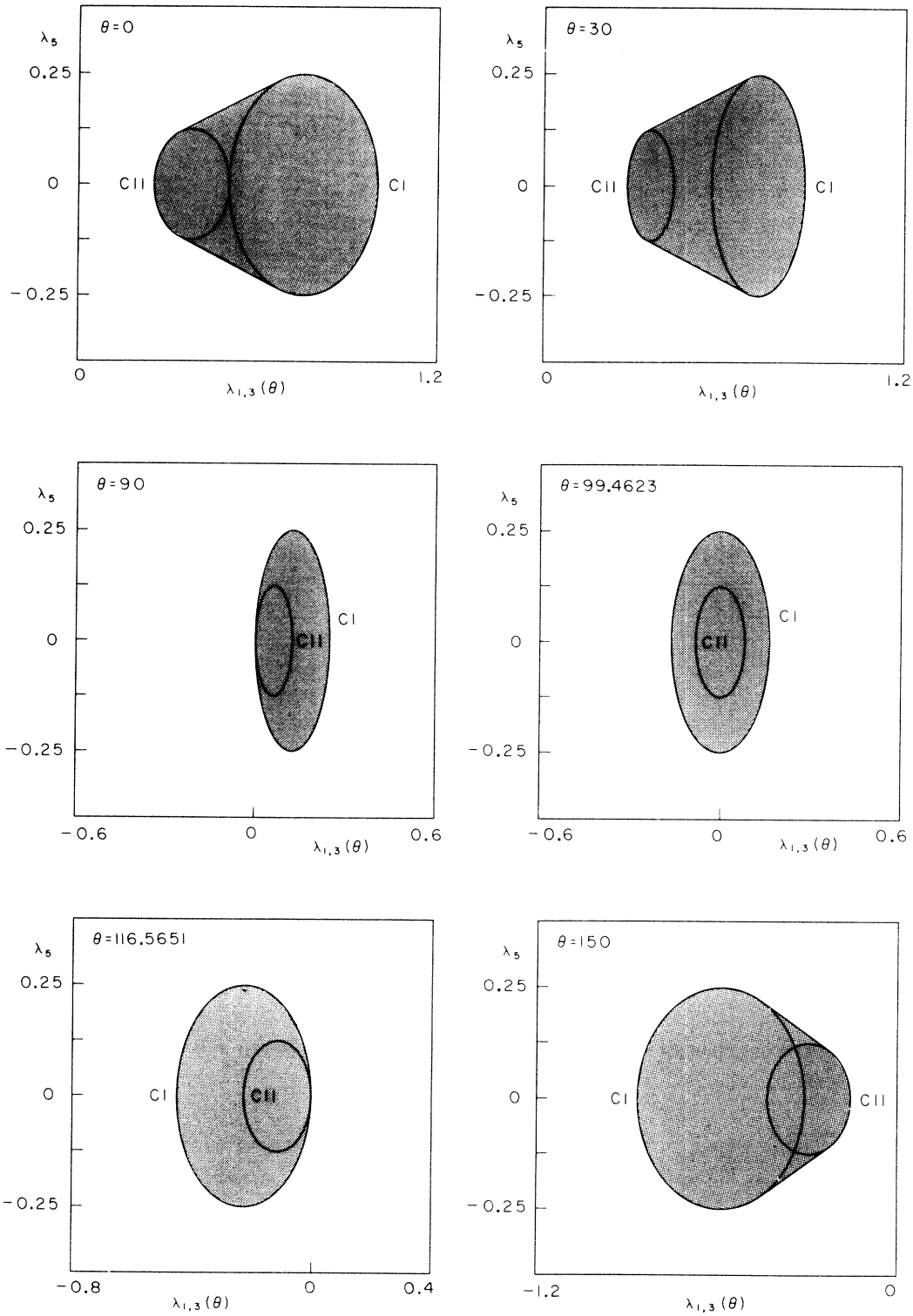

FIG. 7. Orbit space $(\lambda_5, \lambda_1 \cos\theta + \lambda_3 \sin\theta)$ for FD5.

$D64d$ from others. Images $D128a$ and $D64b$ are distinguished from each other at the tenth degree. Tolédano and Tolédano[4] missed two images, $D64b$ and $D64d$, for f_2.

Only phases with maximal isotropy subgroups are realized for images $D128a$, $D64b$, and $D64d$. However, in the case of image $D64a$, $P11$ belongs to an orbit $C8$ corresponding to a submaximal isotropy subgroup. In the case of image $D32a$, $P4$ belongs to $C2$ and $P11$ to $C8$, both of which correspond to submaximal isotropy subgroups. Since the points $P1$, $P3$, $P4$, and $P11$ correspond to the maximal isotropy subgroups of the largest of the five images, the Michel-Radicati conjecture is intact but the Ascher conjecture is violated.

TABLE X. (a) "Phase diagram" for FD5. (b) The limiting angles $\xi_L(\theta)$ to be used in (a). Note that ξ_L is not defined in the interval $90° < \theta < \tan^{-1}(-2)$. All angles are in degrees.

(a)

Octant		Phase	Region
$A_5>0,\ A_{1,3}>0$	$0°<\theta<90°$	$C1$	$0<\xi<\xi_L$
and		$C11$	$\xi_L<\xi$
$A_5<0,\ A_{1,3}>0$	$90°<\theta<180°$	$C1$	everywhere
$A_5>0,\ A_{1,3}<0$	$0°<\theta<116.56°$	$C1$	everywhere
and	$116.56°<\theta<180°$	$C1$	$0<\xi<\xi_L$
$A_5<0,\ A_{1,3}<0$		$C11$	$\xi_L<\xi$

(b)

θ	$\xi_L(\theta)$	θ	$\xi_L(\theta)$
0.0	19.4712	85.0	57.4296
5.0	19.1566	89.0	74.9563
10.0	18.9913	89.995	88.9296
15.0	18.9691	116.65	85.5898
20.0	19.0892	120.0	62.6322
25.0	19.3561	125.0	49.0588
30.0	19.7800	130.0	40.8673
35.0	20.3778	135.0	35.2644
40.0	21.1749	140.0	31.2069
45.0	22.2077	145.0	28.1641
50.0	23.5283	150.0	25.8293
55.0	25.2117	155.0	24.0119
60.0	27.3678	160.0	22.5871
65.0	30.1628	165.0	21.4707
70.0	33.8594	170.0	20.6044
75.0	38.9000	175.0	19.9474
80.0	46.1123	180.0	19.4712

VI. FD4—$(D_2;D_2)^*$: IMAGES $D64c$ AND $D32b$

The free energy to the fourth degree is given by

$$G=\frac{a}{2}I_2+\tfrac{1}{4}(A_0I_2^2+A_1I_1^{(4)}+A_3I_3^{(4)}+A_4I_4^{(4)})$$

$$=\frac{a}{2}I_2+\tfrac{1}{4}\{A_0I_2^2+A_1I_1^{(4)}$$

$$+A_{3,4}[\cos(\theta)I_3^{(4)}+\sin(\theta)I_4^{(4)}]\}\ , \qquad (11)$$

where $A_{3,4}=\pm(A_3^2+A_4^2)^{1/2}$, $\tan\theta=A_4/A_3$, $0°\le\theta\le180°$. The orbit spaces at several representative angles θ are depicted in Fig. 6. The stable phases are listed in Table IX.

The images $D64c$ and $D32b$ are distinguished at the sixth-degree expansion of the free energy. The orbit point $P11$ corresponds to a maximal isotropy subgroup in the case of image $D64c$ but belongs to an orbit $C8$ corre-

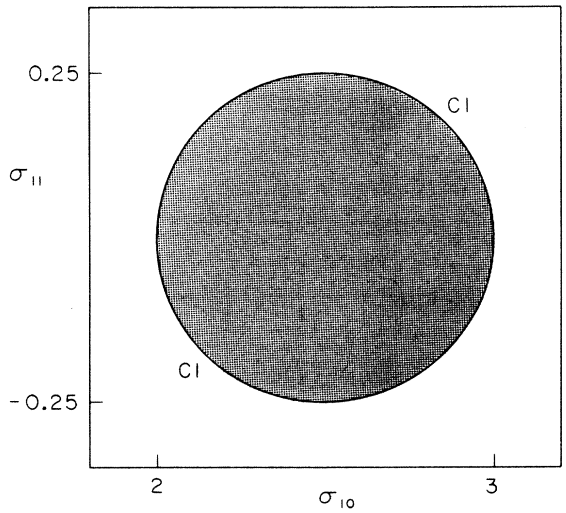

FIG. 8. Orbit space $(\sigma_{11},\sigma_{10})$ for images $D96d$ and $D24b$.

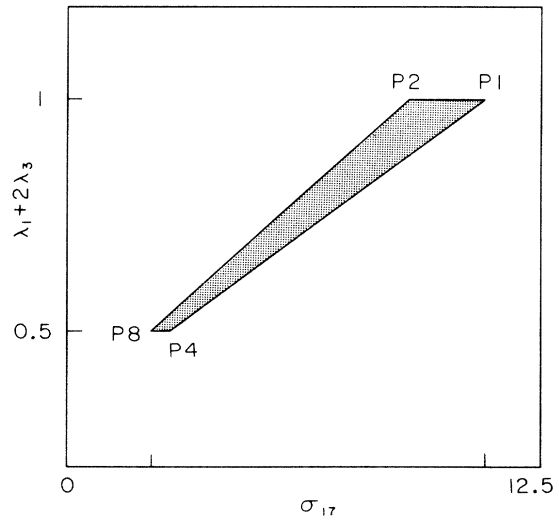

FIG. 9. Orbit space $(\lambda_1+2\lambda_3,\sigma_{17})$ for images $D144a$, $D72a$, and $D72b$.

sponding to a submaximal isotropy subgroup in the case of image $D32b$. Thus the Ascher conjecture is violated but not the Michel-Radicati conjecture.

VII. FD5—$(C_8/C_4;D_4/D_2)$: IMAGE $D32e$

The free energy to the fourth degree is given by

$$G=\frac{a}{2}I_2+\tfrac{1}{4}(A_0I_2^2+A_1I_1^{(4)}+A_3I_3^{(4)}+A_5I_5^{(4)})$$

$$=\frac{a}{2}I_2+\tfrac{1}{4}\{A_0I_2^2+A_{1,3}[\cos(\theta)I_1^{(4)}+\sin(\theta)I_3^{(4)}]$$

$$+A_5I_5^{(4)}\}\ , \qquad (12)$$

where $A_{1,3}=\pm(A_1^2+A_3^2)^{1/2}$, $\tan\theta=A_3/A_1$, $0°\le\theta\le 180°$. The orbit spaces at several representative angles θ are depicted in Fig. 7. The stable phases are listed in Table X(a) and the limiting angle ξ_L at each θ is listed in Table X(b). The angle ξ is defined as

$$\tan\xi=\left|\frac{A_{1,3}}{A_5}\right|\ .$$

The Michel-Radicati conjecture is intact. In Ref. 4 this image was missed and in Ref. 12 it was shown to have a stable fixed point in the renormalization-group flow.

VIII. FD8—$(D_2\times D_2)$: IMAGE $D96d$ AND $D24b$

The free energy to the sixth degree is given by

$$G=\frac{a}{2}I_2+\tfrac{1}{4}A_0I_2^2+\tfrac{1}{6}(B_0I_2^3+B_1I_{10}^{(6)}+B_2I_{11}^{(6)}+\cdots)\ . \qquad (13)$$

At the fourth degree the above free energy is isotropic and thus insufficient to single out a particular direction. Thus we have expanded the free energy up to the sixth degree. The terms omitted in the dots belong to image $D24b$. The orbit space $(\sigma_{10},\sigma_{11})$ is depicted in Fig. 8, where we have defined the orbit parameters $\sigma_i\equiv I_i^{(6)}/I_2^3$. Since the free energy (13) is monotonic in σ_i the absolute minimum occurs again on the orbit space boundary. Thus only the phase $C1$ is realized. Tolédano and Tolédano[4] listed two phases (I,II) for f_6, which are equivalent according to our computation.

Image $D24b$ yields eight linearly independent (but algebraically dependent) sixth-degree invariant polynomials. However, detail analysis is not needed in this case. Only one phase is available at lower temperature.

TABLE XI. "Phase diagram" for FD12.

Quadrant	Phase	Region
$A'_{1,3}>0,\ A'_{4,2}>0$	$P5,P6$	everywhere
$A'_{1,3}>0,\ A'_{4,2}<0$	$P11,P13$	everywhere
$A'_{1,3}<0,\ A'_{4,2}>0$	$P1$	everywhere
$A'_{1,3}<0,\ A'_{4,2}<0$	$P1$	$-2A'_{1,3}+A'_{4,2}>0$
	$P11,P13$	$-2A'_{1,3}+A'_{4,2}<0$

IX. FD11—$(D_\infty\times D_\infty)^*$: IMAGES $D144a$, $D72a$, AND $D72b$

The free energy to the sixth-degree is given by

$$G=\frac{a}{2}I_2+\tfrac{1}{4}[A_0I_2^2+A'_{1,3}(I_1^{(4)}+2I_3^{(4)})]$$

$$+\tfrac{1}{6}[B_0I_2^3+B_1I_2(I_1^{(4)}+2I_3^{(4)})+B_2I_{17}^{(6)}]\ . \qquad (14)$$

The orbit space relevant to the fourth-degree free energy is the projection of that of image $D128a$ onto the dotted line in Fig. 5. At the fourth degree the phases $P1$, $P2$, and $C1$ yield the same absolute minimum and so do the phases $P4$, $P8$, $C10$, and $C11$.

For image $D72b$ a quartic potential is sufficient if we just need to distinguish the two phases $C1$ and $C11$. However, for the other two images it is essential to include the sixth-degree terms in the free energy. The orbit space $(\lambda_1+2\lambda_3,\sigma_{17})$ is depicted in Fig. 9. A general sixth-degree potential in the form of Eq. (14) has been treated in Ref. 20, where the procedure for obtaining the phase diagram was illustrated in the case of $BaTiO_3$. The contour is the same as in Ref. 20. Only the orbit space needs to be replaced. Due to the concavity of the contour, only the orbits $P1$, $P2$, $P4$, and $P8$ can yield the absolute minimum in any region of the coupling constant space $(A'_{1,3},B_1,B_2)$. To obtain the phase diagram, we compare the absolute minimum value, Eq. (10) of Ref. 20 at two competing phases. Tolédano and Tolédano[4] missed two images $D144a$ and $D72a$ and thus listed only two phases $C1$ and $C11$ of f_7.

Image $D72b$ is distinguished at the sixth degree and the images $D144a$ and $D72a$ begin to have different free energies at the eighth degree.

Since the orbit $P4$ belongs to $C2$ and $P8$ to $C4$ in the case of image $D72a$, the Ascher conjecture is violated. But the Michel-Radicati conjecture holds.

X. FD12—$(D_2\times D_\infty)$: IMAGES $D48e$ AND $D24d$

The free energy to the fourth-degree is given by

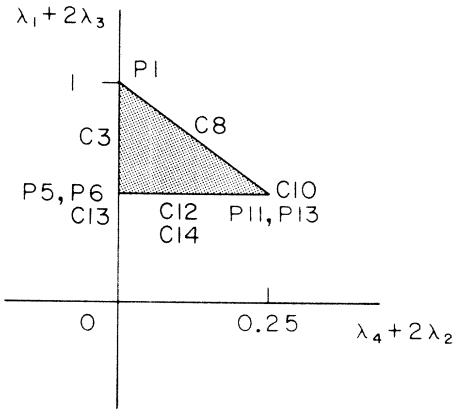

FIG. 10. Orbit space $(\lambda_1+2\lambda_3,\lambda_4+2\lambda_2)$ for FD12.

$$G=\frac{a}{2}I_2+\tfrac{1}{4}[A_0I_2^2+A'_{1,3}(I_1^{(4)}+2I_3^{(4)})$$
$$+A'_{4,2}(I_4^{(4)}+2I_2^{(4)})]\ . \quad (15)$$

The orbit space is depicted in Fig. 10. Despite the additional invariant polynomial $I_4^{(4)}+2I_2^{(4)}$, the degeneracy between pairs of phases ($P5$,$P6$) and ($P11$,$P13$) is not lifted. Inclusion of the sixth-degree terms, $I_{21}^{(6)}$ and $I_{23}^{(6)}$, in the free energy will lift the degeneracies and five phases ($P1$,$P5$,$P6$,$P11$,$P13$) become well separated. If the sixth-degree terms are strong two more phases, $C3$ and $C8$, will become available also. This is in contrast to the previous result. Tolédano and Tolédano[4] listed six one-dimensional orbits for stable phases. The sixth-degree free energy for the image $D48e$ can be readily minimized using Eq. (10) of Ref. 20 or treating the sixth-degree terms perturbatively depending on the strength of the coupling constants. For image $D24d$ there are many sixth-degree invariant polynomials, and it is quite difficult to obtain the phase diagram. We suffice ourselves by listing the stable phases in Table XI obtained at the fourth degree.

The images $D48e$ and $D24d$ are distinguished at the sixth-degree expansion of the free energy, whereas Tolédano and Tolédano[4] indicated that a twelfth-degree potential was needed to distinguish f_8 from f'_8. The point $P1$ belongs to an orbit $C3$ of a submaximal isotropy subgroup in case of image $D48e$ and to the generic orbit $4D1$ of the *minimal isotropy subgroup* in case of image $D24d$. Thus the Michel-Radicati conjecture is violated.

XI. FD13—($C_4\times D_\infty$): IMAGES $D24c$ AND $D24e$

The free energy to the fourth-degree is given by

$$G=\frac{a}{2}I_2+\tfrac{1}{4}[A_0I_2^2+A'_{1,3}(I_1^{(4)}+2I_3^{(4)})$$
$$+A'_{4,2}(I_4^{(4)}+2I_2^{(4)})+A_6I_6^{(4)}]$$
$$=\frac{a}{2}I_2+\tfrac{1}{4}\{A_0I_2^2+A'[\cos(\theta)(I_1^{(4)}+2I_3^{(4)})$$
$$+\sin(\theta)(I_4^{(4)}+2I_2^{(4)})]+A_6I_6^{(4)}\}\ , \quad (16)$$

where

$$A'=\pm[(A'_{1,3})^2+(A'_{4,2})^2]^{1/2}\ ,$$

$\tan\theta=A'_{4,2}/A'_{1,3}$, $0°\le\theta\le180°$. The orbit spaces at several representative angles θ are depicted in Fig. 11. The stable phases are listed in Table XII(a) and the limiting angle ξ_L at each θ is listed in Table XII(b). The angle ξ is defined as

TABLE XII. (a) "Phase diagram" for FD13. (b) The limiting angles $\xi_L(\theta)$ to be used in (a). Note that ξ_L is not defined in the interval $\tan^{-1}(2)<\theta<90°$. All angles are in degrees.

(a)

Quadrant		Phase	Region
$A_6>0$, $A'>0$	$0°<\theta<90°$	$C11,C12,C14$	everywhere
and	$90°<\theta<180°$	$C11,C12,C14$	$0<\xi<\xi_L$
$A_6<0$, $A'>0$		$C1$	$\xi_L<\xi$
$A_6>0$, $A'<0$	$0°<\theta<63.43°$	$C11,C12,C14$	$0<\xi<\xi_L$
and		$C1$	$\xi_L<\xi$
$A_6<0$, $A'<0$	$63.43°<\theta<180°$	$C11,C12,C14$	everywhere

(b)

θ	$\xi_L(\theta)$	θ	$\xi_L(\theta)$
0.0	14.0362	100.0	36.3199
5.0	14.3933	105.0	29.7075
10.0	14.8875	110.0	25.3811
15.0	15.5423	115.0	22.3393
20.0	16.3914	120.0	20.1039
25.0	17.4844	125.0	18.4134
30.0	18.8948	130.0	17.1122
35.0	20.7355	135.0	16.1021
40.0	23.1881	140.0	15.3183
45.0	26.5651	145.0	14.7168
50.0	31.4587	150.0	14.2676
55.0	39.1842	155.0	13.9501
60.0	53.7940	160.0	13.7505
63.40	86.0016	165.0	13.6608
90.25	79.3723	170.0	13.6774
95.0	47.9054	175.0	13.8009
		180.0	14.0362

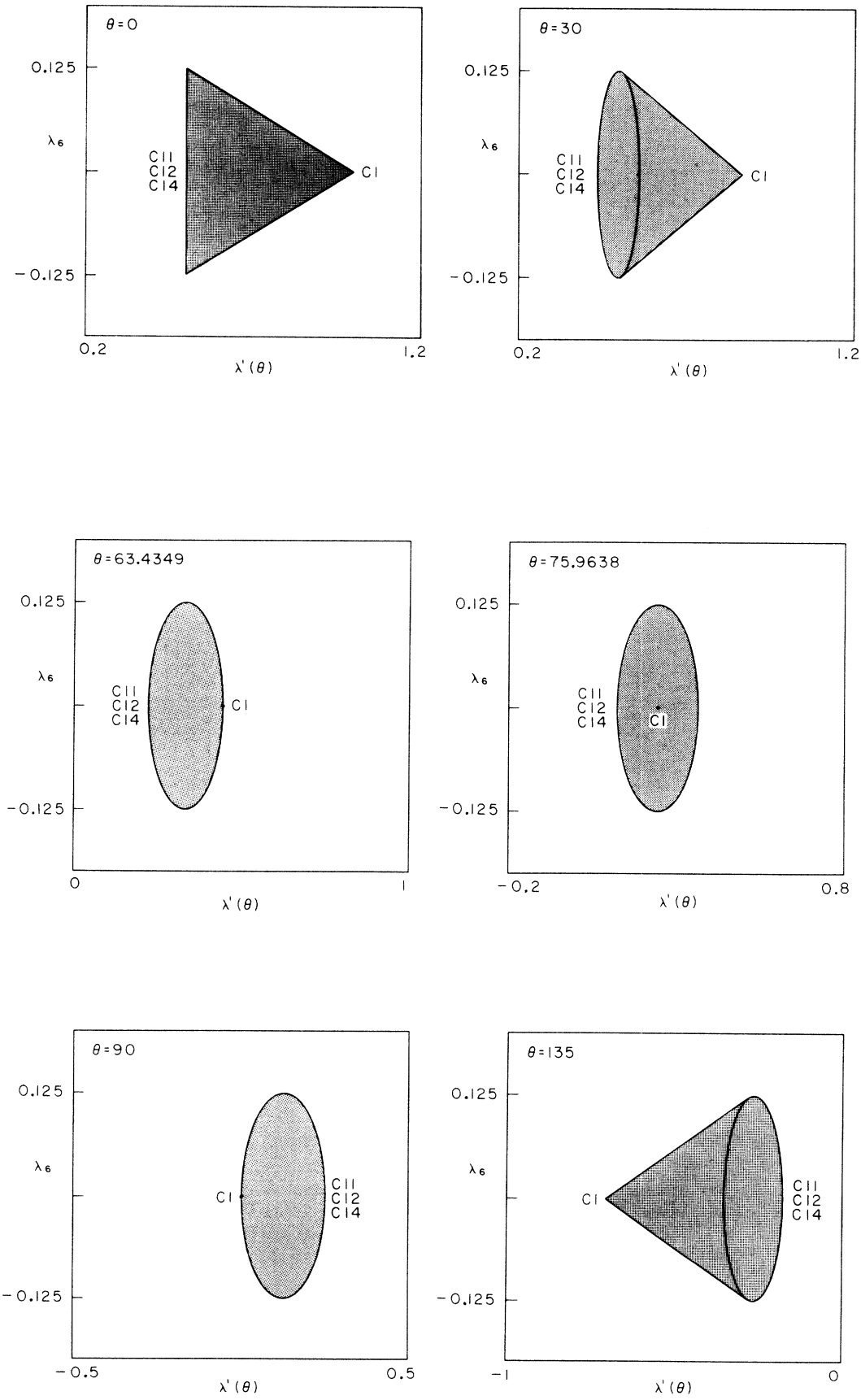

FIG. 11. Orbit space $[\lambda_6, (\lambda_1+2\lambda_3)\cos\theta+(\lambda_4+2\lambda_2)\sin\theta]$ for FD13.

TABLE XIII. "Phase diagram" for FD6. Various limiting angles are defined in Eqs. (18a)–(18f) and their inverses.

		$A_{1,2}>0,\ A_{3,4}>0$	
$0°<\phi<90°$,	$0°<\theta<90°$	$P5$	$-4A_1-A_2+2A_3+2A_4>0$
		$P12$	$-4A_1-A_2+2A_3+2A_4<0$
	$90°<\theta<180°$	$P3$	$-4A_1-A_2-2A_3+2A_4>0$
		$P12$	$-4A_1-A_2-2A_3+2A_4<0$
$90°<\phi<\phi_{C1}$,	$0°<\theta<90°$	$P1$	$-12A_1-A_2+2A_3+2A_4>0$
		$P12$	$-12A_1-A_2+2A_3+2A_4<0$
	$90°<\theta<\theta_{C1}$	$P3$	$-2A_1+A_3<0$
		$P1$	$-2A_1+A_3>0,\ -12A_1-A_2+2A_3+2A_4>0$
		$P12$	$-12A_1-A_2+2A_3+2A_4<0$
	$\theta_{C1}<\theta<180°$	$P3$	$-4A_1-A_2-2A_3+2A_4>0$
		$P12$	$-4A_1-A_2-2A_3+2A_4<0$
$\phi_{C1}<\phi<180°$,	$0°<\theta<90°$	$P1$	everywhere
	$90°<\theta<\min(\theta_{C1},180°)$	$P1$	$-2A_1+A_3>0$
		$P3$	$-2A_1+A_3<0$
	$\theta_{C1}<\theta<180°$	$P3$	$-4A_1-A_2-2A_3+2A_4>0$
		$P12$	$-4A_1-A_2-2A_3+2A_4<0,\ -12A_1-A_2+2A_3+2A_4<0$
		$P1$	$-12A_1-A_2+2A_3+2A_4>0$
		$A_{1,2}>0,\ A_{3,4}<0$	
$0°<\phi<\phi_{C1}$,	$0°<\theta<45°$	$P3$	$-4A_1-A_2-2A_3+2A_4>0$
		$P12$	$-4A_1-A_2-2A_3+2A_4<0$
	$45°<\theta<\min(\theta_{C2},180°)$	$P4$	$-4A_1-A_2+2A_3-2A_4>0$
		$P12$	$-4A_1-A_2+2A_3-2A_4<0$
	$\theta_{C2}<\theta<180°$	$P4$	$-2A_1+A_4<0$
	$90°<\phi<\phi_{C1}$	$P1$	$-2A_1+A_4>0,-12A_1-A_2+2A_3+2A_4>0$
		$P12$	$-12A_1-A_2+2A_3+2A_4<0$
$\phi_{C1}<\phi<\phi_{C2i}$,	$0°<\theta<45°$	$P3$	$-4A_1-A_2-2A_3+2A_4>0$
	$\phi_{C1}<\phi<\phi_{C2a}$	$P12$	$-4A_1-A_2-2A_3+2A_4<0,\ -12A_1-A_2+2A_3+2A_4<0$
		$P1$	$-12A_1-A_2+2A_3+2A_4>0$
	$45°<\theta<135°$	$P4$	$-4A_1-A_2+2A_3-2A_4>0$
	$\phi_{C1}<\phi<\phi_{C2b}$	$P12$	$-4A_1-A_2+2A_3-2A_4<0,\ -12A_1-A_2+2A_3+2A_4<0$
		$P1$	$-12A_1-A_2+2A_3+2A_4>0$
$\phi_{C2i}<\phi<180°$,	$0°<\theta<45°$	$P3$	$-2A_1+A_3<0$
	$\phi_{C2a}<\phi<180°$	$P1$	$-2A_1+A_3>0$
	$45°<\theta<180°$	$P4$	$-2A_1+A_4<0$
	$\max(\phi_{C2b},\phi_{C1})<\phi<180°$	$P1$	$-2A_1+A_4>0$
$0°<\phi<\phi_{C3}$,	$0°<\theta<90°$	$P1$	everywhere
		$A_{1,2}<0,\ A_{3,4}>0$	
	$90°<\theta<\min(\theta_{C3},180°)$	$P1$	$-2A_1+A_3>0$
		$P3$	$-2A_1+A_3<0$
	$\theta_{C3}<\theta<180°$	$P1$	$-12A_1+A_2+2A_3+2A_4>0$
		$P11$	$-12A_1+A_2+2A_3+2A_4<0,\ -4A_1+A_2-2A_3+2A_4<0$
		$P3$	$-4A_1+A_2-2A_3+2A_4>0$
$\phi_{C3}<\phi<90°$,	$0°<\theta<90°$	$P1$	$-12A_1+A_2+2A_3+2A_4>0$
		$P11$	$-12A_1+A_2+2A_3+2A_4<0$
	$90°<\theta<\theta_{C3}$	$P11$	$-12A_1+A_2+2A_3+2A_4<0$
		$P1$	$-12A_1+A_2+2A_3+2A_4>0,\ -2A_1+A_3>0$
		$P3$	$-2A_1+A_3<0$

TABLE XIII. (*Continued*).

		$A_{1,2}<0,\ A_{3,4}>0$	
	$\theta_{C3}<\theta<180°$	$P11$	$-4A_1+A_2-2A_3+2A_4<0$
		$P3$	$-4A_1+A_2-2A_3+2A_4>0$
$90°<\phi<180°$,	$0°<\theta<90°$	$P5$	$-4A_1+A_2+2A_3+2A_4>0$
		$P11$	$-4A_1+A_2+2A_3+2A_4<0$
	$90°<\theta<180°$	$P3$	$-4A_1+A_2-2A_3+2A_4>0$
		$P11$	$-4A_1+A_2-2A_3+2A_4<0$
		$A_{1,2}<0,\ A_{3,4}<0$	
$0°<\phi<\phi_{C4i}$,	$0°<\theta<45°$	$P1$	$-2A_1+A_3>0$
	$0°<\phi<\phi_{C4a}$	$P3$	$-2A_1+A_3<0$
	$45°<\theta<180°$	$P1$	$-2A_1+A_4>0$
	$0°<\phi<\min(\phi_{C4b},\phi_{C3})$	$P4$	$-2A_1+A_4<0$
$\phi_{C4i}<\phi<\phi_{C3}$,	$0°<\theta<45°$	$P1$	$-12A_1+A_2+2A_3+2A_4>0$
	$\phi_{C4a}<\phi<\phi_{C3}$	$P11$	$-12A_1+A_2+2A_3+2A_4<0,\ -4A_1+A_2-2A_3+2A_4<0$
		$P3$	$-4A_1+A_2-2A_3+2A_4>0$
	$45°<\theta<135°$	$P1$	$-12A_1+A_2+2A_3+2A_4>0$
	$\phi_{C4b}<\phi<\phi_{C3}$	$P11$	$-12A_1+A_2+2A_3+2A_4<0,\ -4A_1+A_2+2A_3-2A_4<0$
		$P4$	$-4A_1+A_2+2A_3-2A_4>0$
$\phi_{C3}<\phi<180°$,	$0°<\theta<45°$	$P11$	$-4A_1+A_2-2A_3+2A_4<0$
		$P3$	$-4A_1+A_2-2A_3+2A_4>0$
	$45°<\theta<\min(\theta_{C4},180°)$	$P11$	$-4A_1+A_2+2A_3-2A_4<0$
		$P4$	$-4A_1+A_2+2A_3-2A_4>0$
	$\theta_{C4}<\theta<180°$	$P11$	$-12A_1+A_2+2A_3+2A_4<0$
		$P1$	$-12A_1+A_2+2A_3+2A_4>0,\ -2A_1+A_4>0$
		$P4$	$-2A_1+A_4<0$

$$\tan\xi=\left|\frac{A'}{A_6}\right| .$$

The phases $C12$ and $C14$ are not distinguished with the fourth-degree free energy. Thus we are again compelled to include the sixth-degree terms $(I_{21}^{(6)},I_{23}^{(6)},I_{24}^{(6)})$ to lift the degeneracy between phases with maximal isotropy subgroups in the case of image $D24c$. However, in the case of image $D24e$, the two phases $C1$ and $C11$ are distinguished at the fourth-degree, though the order parameter components cannot be specified to the last detail for $C1$, which the sixth-degree terms should provide. But a twelfth-degree potential is not needed as indicated in Ref. 4.

Although we have chosen the basis of the two images in such a way that the fourth-degree potentials are identical, the images $D24c$ and $D24e$ are not group-subgroup related as we can see in the tree diagram Fig. 1. Thus the Ascher conjecture need not be checked. In the case of image $D24c$ the point $C1$ does not belong to an orbit of a maximal isotropy subgroup but corresponds to the *minimal isotropy subgroup,* leading to the violation of the Michel-Radicati conjecture.

XII. FD6—($D_2\times D_2$): IMAGE $D32c$

The free energy to the fourth degree is given by

$$G=\frac{a}{2}I_2+\tfrac{1}{4}(A_0I_2^2+A_1I_1^{(4)}+A_2I_2^{(4)}+A_3I_3^{(4)}+A_4I_4^{(4)})$$
$$=\frac{a}{2}I_2+\tfrac{1}{4}\{A_0I_2^2+A_{1,2}[\cos(\phi)I_1^{(4)}+\sin(\phi)I_2^{(4)}]$$
$$+A_{3,4}[\cos(\theta)I_3^{(4)}+\sin(\theta)I_4^{(4)}]\} , \qquad (17)$$

where $A_{1,2}=\pm(A_1^2+A_2^2)^{1/2}$, $\tan\phi=A_2/A_1$, $0°\le\phi\le180°$, and $A_{3,4}=\pm(A_3^2+A_4^2)^{1/2}$, $\tan\theta=A_4/A_3$, $0°\le\theta\le180°$.

It is not in general an easy task to analyze a potential with more than four independent invariant polynomials. We have included this image because it could be analyzed without much difficulty. The orbit spaces at several

TABLE XIV. Examples of maximal symmetry breaking. Space-group representations and their isotropy subgroups are listed.

Image	$D24c$		$D24d$	
Irrep	$P_3\oplus P_3^*$		$P_2\oplus P_3$	
Space group	T_d^3	($I\bar{4}3m$; No. 217)	T_h^5	($Im3$; No. 204)
$C12/C10$	D_{2d}^9	($I\bar{4}m2$; No. 119)	D_{2h}^{23}	($Fmmm$; No. 69)
$C14/C13$	D_{2d}^{10}	($I\bar{4}c2$; No. 120)	D_{2h}^{24}	($Fddd$; No. 70)
$C14/C13$	D_{2d}^{10}	($I\bar{4}c2$; No. 120)	D_{2h}^{24}	($Fddd$; No. 70)
$4D1$	D_2^7	($F222$; No. 22)	D_2^7	($F222$; No. 22)

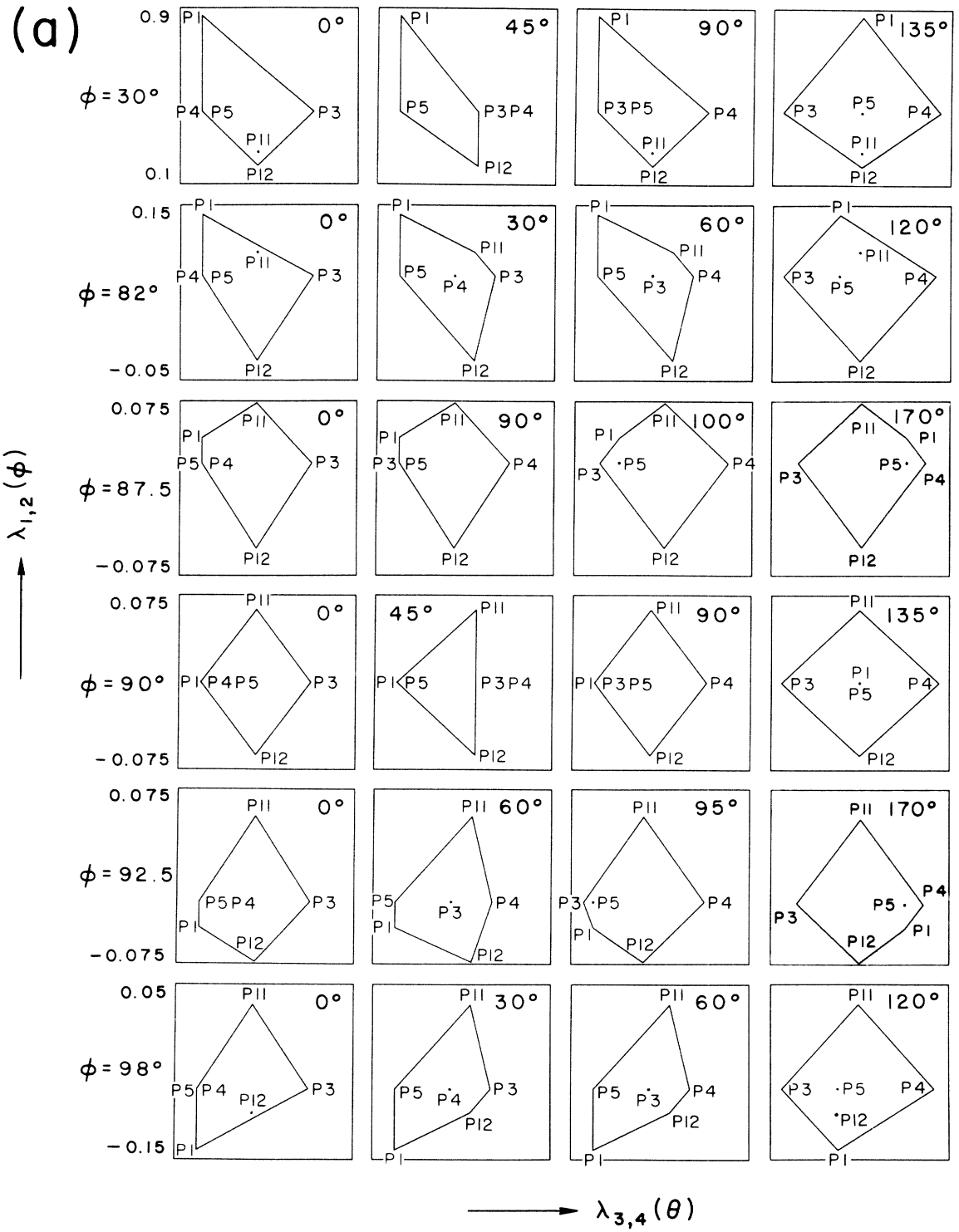

FIG. 12. (a) Orbit space $(\lambda_1\cos\phi+\lambda_2\sin\phi, \lambda_3\cos\theta+\lambda_4\sin\theta)$ for FD6 is sketched at various angles (ϕ,θ). θ is specified in each frame. The scales of the horizontal axis are $-0.05<x<0.35$ for $0°<\theta<95°$; $-0.1<x<0.3$ for $\theta=100°$, $-0.15<x<0.25$ for $\theta=120°$, $-0.2<x<0.2$ for $\theta=135°$, and $-0.3<x<0.1$ for $\theta=170°$. (b) Subregions in the coupling constant space with the corresponding stable phases for each quadrant of $(A_{1,2},A_{3,4})$. In each quadrant the horizontal axis extends $0°\le\theta\le180°$, and for the vertical axis only the portion $60°\le\phi\le120°$ is included to enlarge that portion.

representative angles (ϕ,θ) are depicted in Fig. 12(a). The stable phases are listed in Table XIII. Considering the complexity of the stability regions we provided Fig. 12(b). The limiting angles ϕ_{C1}, ϕ_{C2a}, ϕ_{C2b}, ϕ_{C3}, ϕ_{C4a}, ϕ_{C4b} are given by

$$\tan(\phi_{C1})=-12\ , \tag{18a}$$

$$\tan(\phi_{C2a})=4\tan\theta-8\ , \tag{18b}$$

$$\tan(\phi_{C2b})=4\cot\theta-8\ , \tag{18c}$$

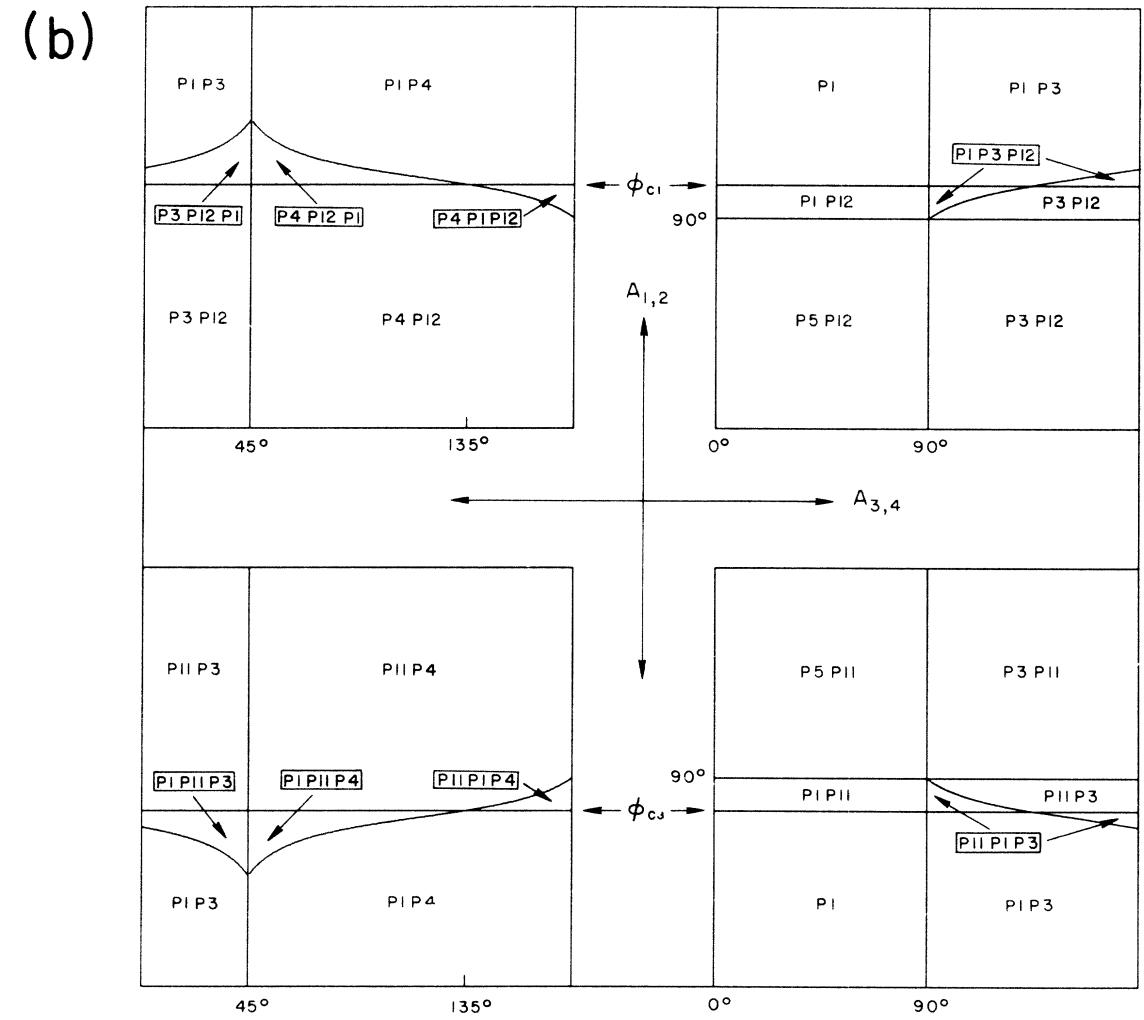

FIG. 12. (*Continued*).

$$\tan(\phi_{C3}) = 12 , \tag{18d}$$

$$\tan(\phi_{C4a}) = 8 - 4\tan\theta , \tag{18e}$$

$$\tan(\phi_{C4b}) = 8 - 4\cot\theta . \tag{18f}$$

The limiting angles θ_{C1}, θ_{C2}, θ_{C3}, and θ_{C4} are given as inverse functions of Eqs. (18b), (18c), (18e), and (18f), respectively. All maximal symmetry phases are realized with the quartic potential and the Michel-Radicati conjecture is not violated.

XIII. SUMMARY AND CONCLUSIONS

We have obtained the phase diagrams for ten types of quartic potentials condensed from 23 images of four-dimensional active space-group representations corresponding to points of symmetry. Our list of phases agrees with that obtained by Tolédano and Tolédano,[4] except for the following cases:

(i) FD3—images $D64b$ and $D64d$; they missed.

(ii) FD5—image $D32e$; they missed.

(iii) FD8—image $D96d$; their list contains a pair of equivalent phases.

(iv) FD11—images $D144a$ and $D72a$; they missed these images and consequently missed four phases, $P1$, $P2$, $P4$, and $P8$.

(v) FD12—image $D48e$; their list of stable phases is wrong and only a sixth-degree potential is sufficient to lift degeneracies between phases.

(vi) FD13—image $D24c$ and $D24e$; a sixth-degree potential is sufficient to lift degeneracies between phases.

Although the degeneracies between phases can be lifted by sixth-degree terms, we noticed that in most cases the free energy needs to be expanded to quite a high degree to distinguish different images that are group-subgroup related.

Four (FD1, FD3, FD5, and FD11) of the five quartic potentials having stable fixed points[12] in the renormalization-group flow have been analyzed in this paper. Thus physical systems described by these four quartic potentials can undergo continuous phase transitions regardless of fluctuations. The remaining quartic potential with the centralizer $(Y/C2;Y^*/C2)^*$ does not correspond to any space-group representation because icosahedral symmetry cannot be a symmetry of a three-dimensional crystal lattice.

It is interesting that phase transitions induced by order parameters transforming according to two images, $D24c$ and $D24d$, can yield the *minimal* symmetry. We include the space-group changes for these two cases in Table XIV.

[1]J. S. Kim, D. M. Hatch, and H. T. Stokes, Phys. Rev. B **33**, 1774 (1986).

[2]Yu. M. Gufan and V. P. Sakhnenko, Zh. Eksp. Teor. Fiz. **63**, 1909 (1972) [Sov. Phys.—JETP **36**, 1009 (1973)].

[3]L. Michel and J. Mozrzymas, in *Group Theoretical Methods in Physics,* Vol. 79 of *Lecture Notes in Physics,* edited by P. Kramer and A. Rieckers (Springer-Verlag, Berlin, 1978), p. 447.

[4]J. C. Tolédano and P. Tolédano, Phys. Rev. B **21**, 1139 (1980).

[5]S. L. Altmann, *Induced Representations in Crystals and Molecules* (Academic, London, 1977); J. L. Birman, *Theory of Crystal Space Groups and Lattice Dynamics* (Springer-Verlag, Berlin, 1974); G. Burns and A. M. Glazer, *Space Groups for Solid State Scientists* (Academic, New York, 1978); C. J. Bradley and A. P. Cracknell, *The Mathematical Theory of Symmetry in Solids* (Clarendon, Oxford, 1972); G. Ya. Lyubarskii, *The Application of Group Theory in Physics* (Pergamon, New York, 1960), Chap. VII.

[6]A. P. Cracknell, B. L. Davis, S. C. Miller, and W. F. Love, *Kronecker Product Tables* (JFI/Plenum, New York, 1979).

[7]O. V. Kovalev, *Irreducible Representations of Space Groups* (Gordon and Breach, New York, 1965); J. Zak, A. Cacher, H. Glück, and Y. Gur, *The Irreducible Representations of Space Groups* (Benjamin, New York, 1969).

[8]J. S. Kim, Nucl. Phys. B **196**, 285 (1982); **197**, 174 (1982); S. Frautschi and J. S. Kim, *ibid.* **196**, 301 (1982).

[9]H. T. Stokes and D. M. Hatch (unpublished).

[10]J. S. Kim, J. Math. Phys. **25**, 1694 (1984).

[11]L. Michel, J. C. Tolédano, and P. Tolédano, in *Symmetries and Broken Symmetries in Condensed Matter Physics,* edited by N. Boccara (IDSET, Paris, 1981), p. 261.

[12]J. C. Tolédano, L. Michel, P. Tolédano, and E. Brézin, Phys. Rev. B **31**, 7171 (1985).

[13]E. Ascher, J. Phys. C **10**, 1365 (1977).

[14]L. Michel and L. A. Radicati, in *Evolution of Particle Physics,* edited by M. Conversi (Academic, New York, 1970), p. 191.

[15]H. T. Stokes, D. M. Hatch, and J. S. Kim (unpublished).

[16]*International Tables for Crystallography,* edited by T. Hahn (Reidel, Dordrecht, 1983), Vol. A.

[17]We have been using the term orbit space (see Ref. 8) for the *localized region of "angles"* obtained from dimensionless ratios of basic invariant polynomials to the appropriate power of the quadratic invariant I_2. A complete set of $(n-1)$ different angles and I_2 specify an orbit. Thus our orbit space is a projected orbit space and specifies an orbit as much in detail as a free energy of a given degree.

[18]G. E. Bredon, *Introduction to Compact Transformation Groups* (Academic, New York, 1972); L. Michel, in *Regards sur la Physique Contemporaine* (Centre National de la Recherche Scientifique, Paris, 1980), pp. 157–203; M. Abud and G. Sartori, Ann. Phys. (N.Y.) **150**, 307 (1983).

[19]J. L. Birman, Phys. Rev. Lett. **17**, 1216 (1966); F. E. Goldrich and J. L. Birman, Phys. Rev. **167**, 528 (1968); M. V. Jaric and J. L. Birman, Phys. Rev. B **16**, 2564 (1977); M. V. Jaric, *ibid.* **23**, 3460 (1981).

[20]J. S. Kim, Phys. Rev. B **31**, 1433 (1985).

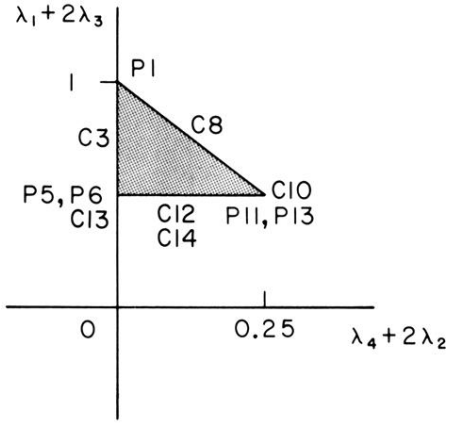

FIG. 10. Orbit space $(\lambda_1+2\lambda_3, \lambda_4+2\lambda_2)$ for FD12.

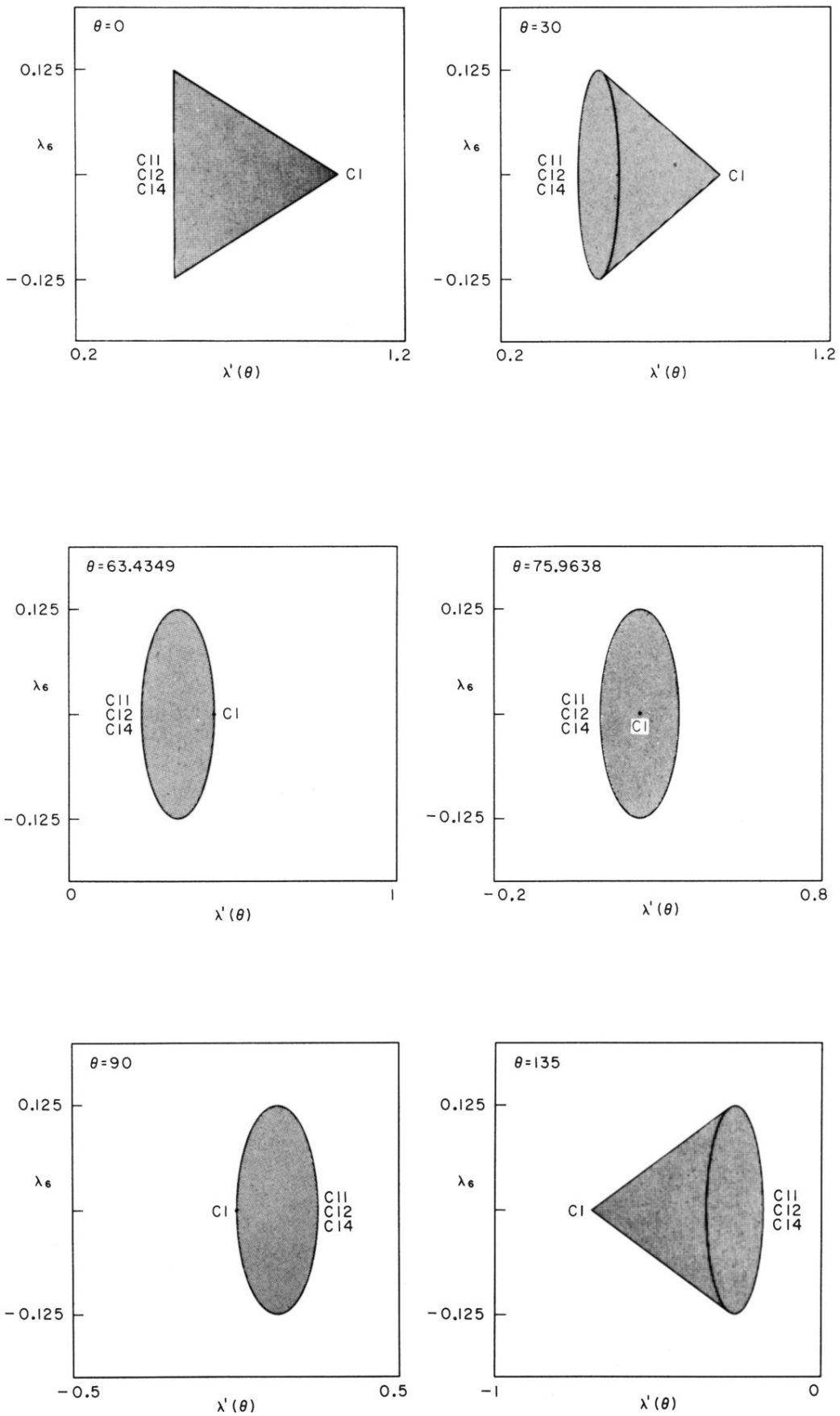

FIG. 11. Orbit space $[\lambda_6, (\lambda_1+2\lambda_3)\cos\theta+(\lambda_4+2\lambda_2)\sin\theta]$ for FD13.

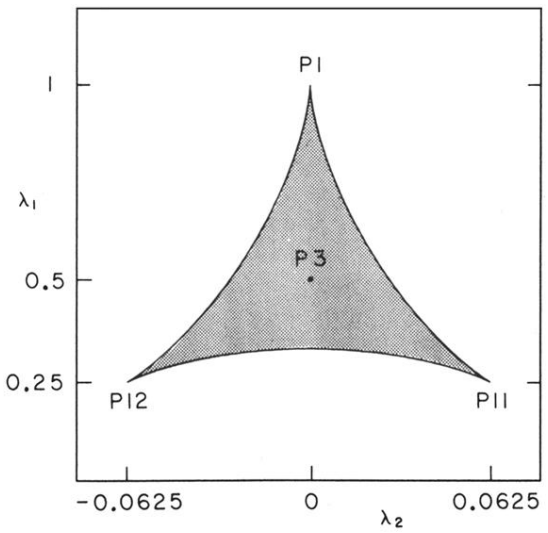

FIG. 4. Orbit space (λ_1, λ_2) for FD2.

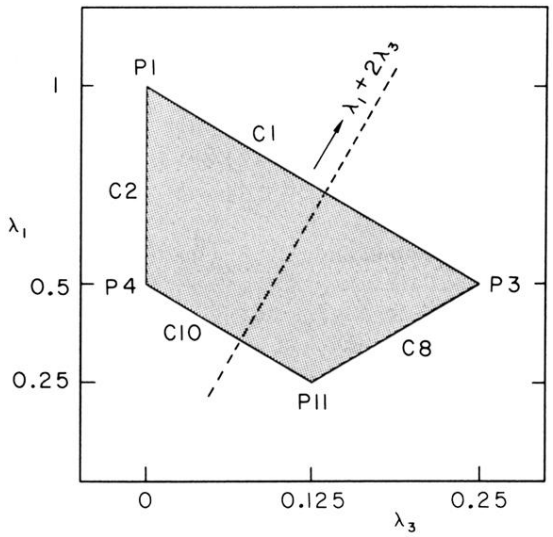

FIG. 5. Orbit space (λ_1,λ_3) for FD3.

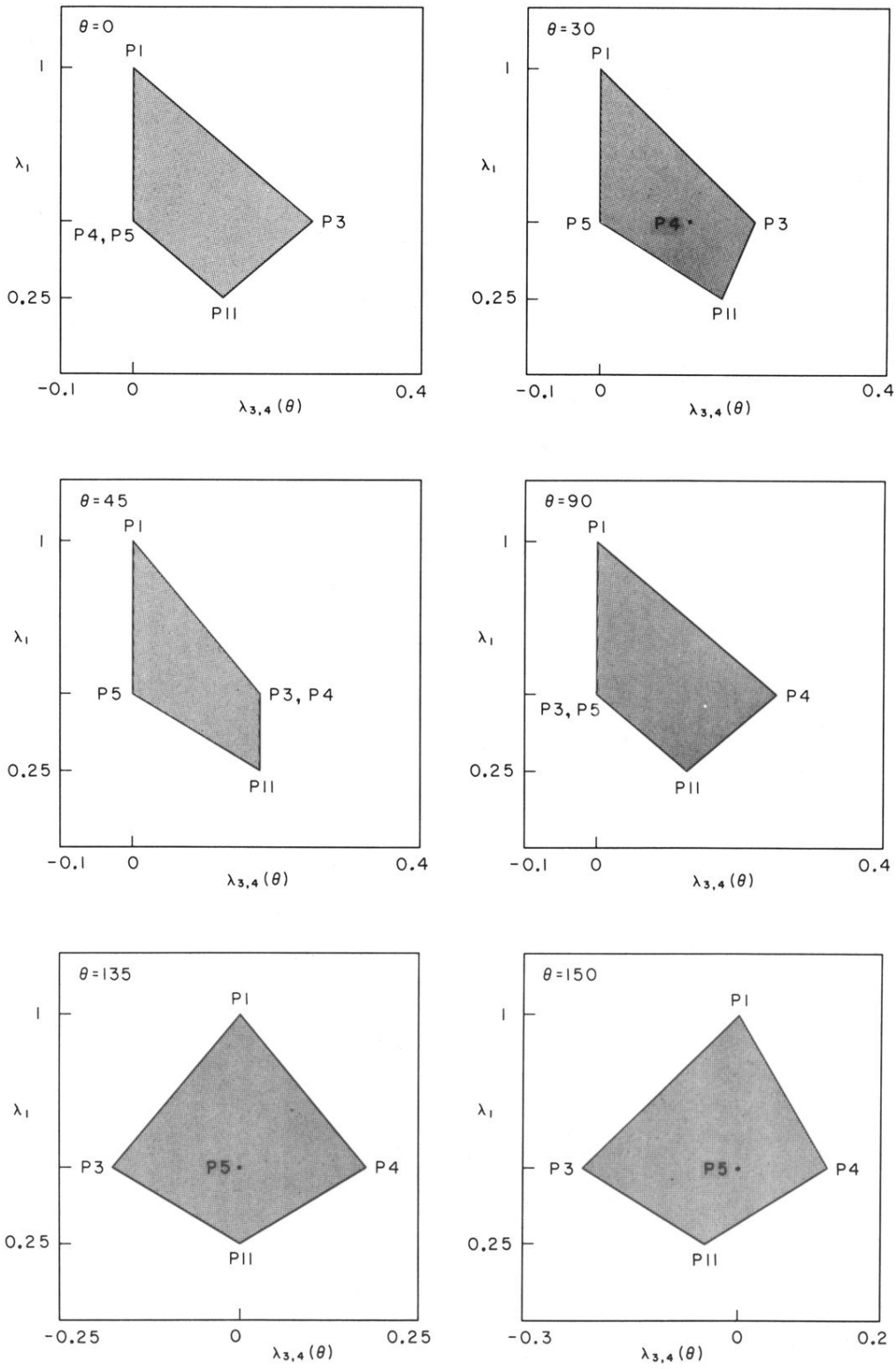

FIG. 6. Orbit space $(\lambda_1, \lambda_3 \cos\theta + \lambda_4 \sin\theta)$ for FD4.

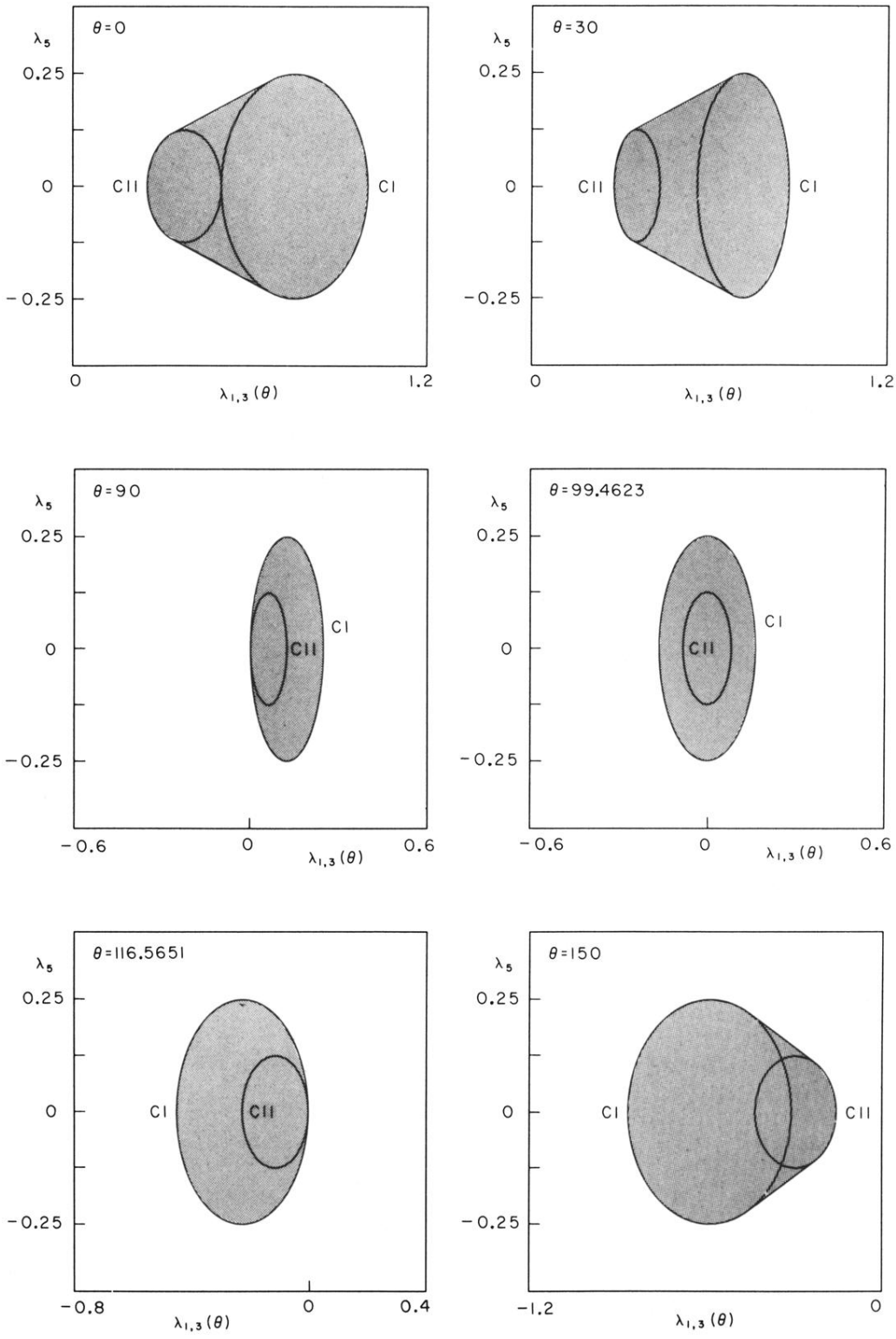

FIG. 7. Orbit space $(\lambda_5, \lambda_1 \cos\theta + \lambda_3 \sin\theta)$ for FD5.

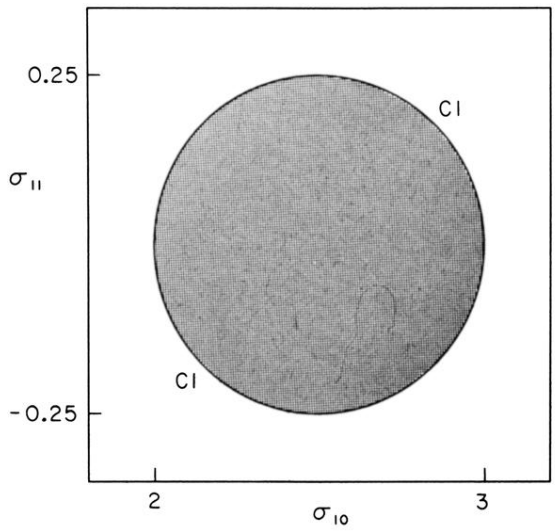

FIG. 8. Orbit space $(\sigma_{11},\sigma_{10})$ for images *D*96*d* and *D*24*b*.

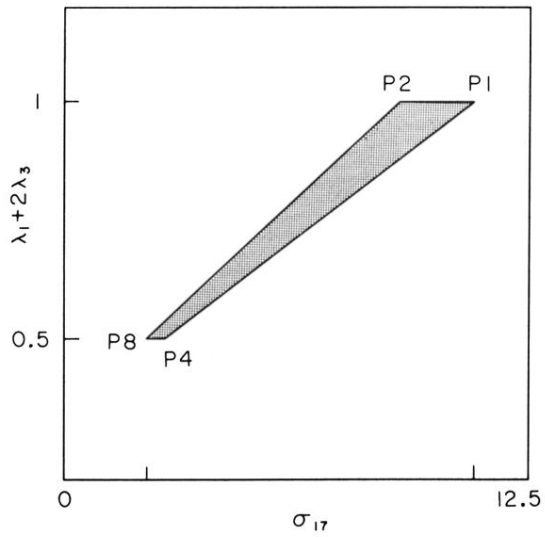

FIG. 9. Orbit space $(\lambda_1+2\lambda_3, \sigma_{17})$ for images *D*144*a*, *D*72*a*, and *D*72*b*.